

1 **Mitochondrial respiratory states and rates:**
2 **Building blocks of mitochondrial physiology Part 1**
3

4 **COST Action CA15203 MitoEAGLE preprint** Version: 2018-04-20(38)

5 Corresponding author: Gnaiger E

6 Co-authors:

7 Aasander Frostner E, Abumrad NA, Acuna-Castroviejo D, Ahn B, Ali SS, Alves MG, Amati
8 F, Aral C, Arandarčikaitė O, Bailey DM, Bajpeyi S, Bakker BM, Bastos Sant'Anna Silva AC,
9 Battino M, Bazil J, Beard DA, Bednarczyk P, Ben-Shachar D, Bergdahl A, Bernardi P,
10 Bishop D, Blier PU, Boetker HE, Boros M, Borsheim E, Borutaitė V, Bouillaud F, Boutbir J,
11 Breton S, Brown DA, Brown GC, Brown RA, Brozinick JT, Buettner GR, Burtscher J,
12 Calabria E, Calbet JA, Calzia E, Cannon DT, Canto AC, Cardoso LHD, Carvalho E, Casado
13 Pinna M, Cassina AM, Castro L, Cavalcanti-de-Albuquerque JP, Cervinkova Z, Chang SC,
14 Chaurasia B, Chen Q, Chicco AJ, Chinopoulos C, Chowdhury SK, Clementi E, Coen PM,
15 Coker RH, Collin A, Crisóstomo L, Darveau CA, Das AM, Dash RK, Davis MS, De Palma C,
16 Dembinska-Kiec A, Dias TR, Distefano G, Doerrier C, Drahota Z, Dubouchaud H, Duchon
17 MR, Dumas JF, Durham WJ, Dymkowska D, Dyrstad SE, Dzialowski EM, Ehinger J, Elmer
18 E, Endlicher R, Engin AB, Fell DA, Ferko M, Ferreira JCB, Ferreira R, Fessel JP, Filipovska
19 A, Fisar Z, Fischer M, Fisher G, Fisher JJ, Fornaro M, Galkin A, Gan Z, Garcia-Roves PM,
20 Garcia-Souza LF, Garlid KD, Garrabou G, Garten A, Gastaldelli A, Genova ML, Giovarelli
21 M, Gonzalez-Armenta JL, Gonzalo H, Goodpaster BH, Gorr TA, Gourlay CW, Granata C,
22 Grefte S, Gueguen N, Haas CB, Haavik J, Haendeler J, Hamann A, Han J, Hancock CR, Hand
23 SC, Hargreaves IP, Harrison DK, Heales SJR, Hellgren KT, Hepple RT, Hernansanz-Agustin
24 P, Hickey AJ, Hoel F, Holland OJ, Holloway GP, Hoppel CL, Houstek J, Hunger M, Iglesias-
25 Gonzalez J, Irving BA, Iyer S, Jackson CB, Jadiya P, Jang DH, Jang YC, Jansen-Dürr P,
26 Jespersen NR, Jha RK, Jurk D, Kaambre T, Kaczor JJ, Kainulainen H, Kandel SM, Kane DA,
27 Kappler L, Karabatsiakos A, Karkucinska-Wieckowska A, Keijer J, Keppner G, Khamoui AV,
28 Klingenspor M, Komlodi T, Koopman WJH, Kopitar-Jerala N, Kowaltowski AJ, Krajcova A,
29 Krako Jakovljevic N, Kristal BS, Kuang J, Kucera O, Kwak HB, Kwast K, Labieniec-Watala
30 M, Lai N, Land JM, Lane N, Laner V, Lanza IR, Larsen TS, Lavery GG, Lee HK,
31 Leeuwenburgh C, Lemieux H, Lerfall J, Li PA, Liu J, Lucchinetti E, Macedo MP,
32 MacMillan-Crow LA, Makrecka-Kuka M, Malik A, Markova M, Martin DS, Mazat JP,
33 McKenna HT, Menze MA, Meszaros AT, Methner A, Michalak S, Moellering DR, Moiso N,
34 Molina AJA, Montaigne D, Moreau K, Moore AL, Moreira BP, Mracek T, Muntane J,
35 Muntean DM, Murray AJ, Nair KS, Nemec M, Neuffer PD, Neuzil J, Newsom S, Nozickova
36 K, O'Gorman D, Oliveira MF, Oliveira MT, Oliveira PF, Oliveira PJ, Orynbayeva Z,
37 Osiewacz HD, Pak YK, Pallotta ML, Palmeira CM, Parajuli N, Passos JF, Patel HH, Pecina
38 P, Pelna D, Pereira da Silva Grilo da Silva F, Pesta D, Petit PX, Pettersen IKN, Pichaud N,
39 Piel S, Pietka TA, Pino MF, Pirkmajer S, Porter C, Porter RK, Pranger F, Prochownik EV,
40 Pulinilkunnil T, Puskarich MA, Puurand M, Quijano C, Radenkovic F, Radi R, Ramzan R,
41 Rattan S, Reboredo P, Renner-Sattler K, Robinson MM, Roden M, Rohlena J, Rolo AP,
42 Ropelle ER, Røslund GV, Rossiter HB, Rybacka-Mossakowska J, Saada A, Safaei Z, Salin K,
43 Salvadego D, Sandi C, Sanz A, Sazanov LA, Scatena R, Schartner M, Scheibye-Knudsen M,
44 Schilling JM, Schlattner U, Schönfeld P, Schwarzer C, Scott GR, Shabalina IG, Sharma P,
45 Sharma V, Shevchuk I, Siewiera K, Silber AM, Silva AM, Sims CA, Singer D, Skolik R,
46 Smenes BT, Smith J, Soares FAA, Sobotka O, Sokolova I, Sonkar VK, Sparagna GC, Sparks
47 LM, Spinazzi M, Stankova P, Stary C, Stier A, Stocker R, Sumbalova Z, Suravajhala P,
48 Swerdlow RH, Swiniuch D, Szabo I, Szewczyk A, Tanaka M, Tandler B, Tarnopolsky MA,
49 Tavernarakis N, Tepp K, Thyfault JP, Tomar D, Towheed A, Tretter L, Trifunovic A,
50 Trivigno C, Tronstad KJ, Trougakos IP, Tyrrell DJ, Urban T, Valentine JM, Velika B,
51 Vendelin M, Vercesi AE, Victor VM, Vieyra A Villena JA, Vitorino RMP, Vogt S, Volani C,

Votion DM, Vujacic-Mirski K, Wagner BA, Ward ML, Warnsmann V, Wasserman DH,
 Watala C, Wei YH, Wieckowski MR, Williams C, Wohlgemuth SE, Wohlwend M, Wolff J,
 Wüst RCI, Yokota T, Zablocki K, Zaugg K, Zaugg M, Zhang Y, Zhang YZ, Zischka H,
 Zorzano A

Updates and discussion:

http://www.mitoeagle.org/index.php/MitoEAGLE_preprint_2018-02-08

Correspondence: Gnaiger E

Chair COST Action CA15203 MitoEAGLE – <http://www.mitoeagle.org>

*Department of Visceral, Transplant and Thoracic Surgery, D. Swarovski Research
 Laboratory, Medical University of Innsbruck, Innrain 66/4, A-6020 Innsbruck, Austria*

Email: mitoeagle@i-med.ac.at; Tel: +43 512 566796, Fax: +43 512 566796 20

Abstract - Executive summary

1. Introduction – Box 1: In brief: Mitochondria and Bioblasts

2. Oxidative phosphorylation and coupling states in mitochondrial preparations

Mitochondrial preparations

2.1. Respiratory control and coupling

The steady-state

Specification of biochemical dose

Phosphorylation, P_{\gg} , and P_{\gg}/O_2 ratio

Control and regulation

Respiratory control and response

Respiratory coupling control and ET-pathway control

Coupling

Uncoupling

2.2. Coupling states and respiratory rates

Respiratory capacities in coupling control states

LEAK, OXPHOS, ET, ROX

Quantitative relations

2.3. Classical terminology for isolated mitochondria

States 1–5

3. Normalization: flows and fluxes

3.1. Normalization: system or sample

Flow per system, I

Extensive quantities

Size-specific quantities – Box 2: Metabolic flows and fluxes: vectorial and scalar

3.2. Normalization for system-size: flux per chamber volume

System-specific flux, J_{V,O_2}

3.3. Normalization: per sample

Sample concentration, C_{mX}

Mass-specific flux, $J_{O_2/mX}$

Number concentration, C_{NX}

Flow per object, $I_{O_2/X}$

3.4. Normalization for mitochondrial content

Mitochondrial concentration, C_{mtE} , and mitochondrial markers

Mitochondria-specific flux, $J_{O_2/mtE}$

3.5. Evaluation of mitochondrial markers

3.6. Conversion: units

4. Conclusions – Box 3: Recommendations for studies with mitochondrial preparations

References

104 **Abstract** As the knowledge base and importance of mitochondrial physiology to human health
 105 expands, the necessity for harmonizing the terminology concerning mitochondrial respiratory
 106 states and rates has become increasingly apparent. The chemiosmotic theory establishes the
 107 mechanism of energy transformation and coupling in oxidative phosphorylation. The unifying
 108 concept of the protonmotive force provides the framework for developing a consistent
 109 theoretical foundation of mitochondrial physiology and bioenergetics. We follow IUPAC
 110 guidelines on terminology in physical chemistry, extended by considerations on open systems
 111 and irreversible thermodynamics. The concept-driven constructive terminology incorporates
 112 the meaning of each quantity and aligns concepts and symbols to the nomenclature of classical
 113 bioenergetics. In the frame of COST Action MitoEAGLE open to global bottom-up input, we
 114 endeavour to provide a balanced view on mitochondrial respiratory control and a critical
 115 discussion on reporting data of mitochondrial respiration in terms of metabolic flows and fluxes.
 116 Uniform standards for evaluation of respiratory states and rates will ultimately support the
 117 development of databases of mitochondrial respiratory function in species, tissues, and cells.
 118 Clarity of concept and consistency of nomenclature facilitate effective transdisciplinary
 119 communication, education, and ultimately further discovery.

120
 121 *Keywords:* Mitochondrial respiratory control, coupling control, mitochondrial
 122 preparations, protonmotive force, uncoupling, oxidative phosphorylation, OXPHOS,
 123 efficiency, electron transfer, ET; proton leak, LEAK, residual oxygen consumption, ROX, State
 124 2, State 3, State 4, normalization, flow, flux, O₂

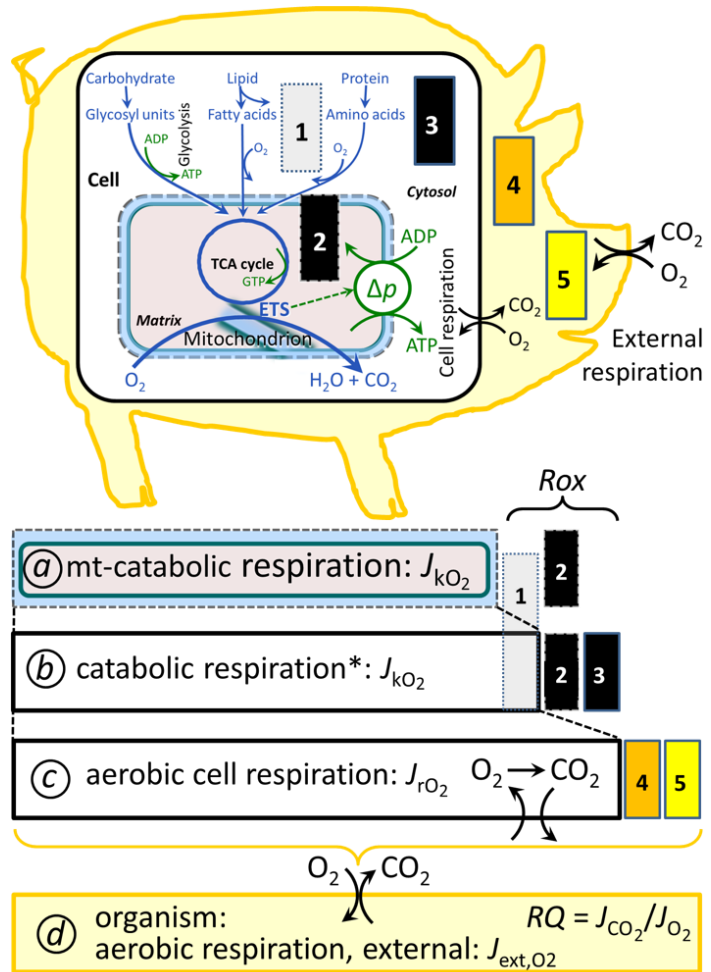
125

126 **Executive summary**

127

- 128 1. In view of the broad implications for health care, mitochondrial researchers face an
 129 increasing responsibility to disseminate their fundamental knowledge and novel
 130 discoveries to a wide range of stakeholders and scientists beyond the group of
 131 specialists. This requires implementation of a commonly accepted terminology
 132 within the discipline and standardization in the translational context. Authors,
 133 reviewers, journal editors, and lecturers are challenged to collaborate with the aim
 134 to harmonize the nomenclature in the growing field of mitochondrial physiology
 135 and bioenergetics, from evolutionary biology and comparative physiology to
 136 mitochondrial medicine.
- 137 2. Aerobic respiration depends on the coupling of phosphorylation (ADP → ATP) to O₂
 138 flux in catabolic reactions. Coupling in oxidative phosphorylation is mediated by
 139 translocation of protons across the inner mitochondrial membrane through proton
 140 pumps generating or utilizing the protonmotive force, that is measured between the
 141 mitochondrial matrix and intermembrane compartment or outer mitochondrial
 142 space. Compartmental coupling distinguishes vectorial oxidative phosphorylation
 143 from glycolytic fermentation as the counterpart of cellular core energy metabolism
 144 (**Figure 1**).
- 145 3. To exclude fermentation and other cytosolic interactions from exerting an effect on the
 146 analysis of mitochondrial metabolism, the barrier function of the plasma membrane
 147 must be disrupted. Selective removal or permeabilization of the plasma membrane
 148 yields mitochondrial preparations—including isolated mitochondria, tissue and
 149 cellular preparations—with structural and functional integrity. Then extra-
 150 mitochondrial concentrations of fuel substrates, ADP, ATP, inorganic phosphate,
 151 and cations including H⁺ can be controlled to determine mitochondrial function
 152 under a set of conditions defined as coupling control states. A concept-driven
 153 terminology of bioenergetics explicitly incorporates in its terms and symbols
 154 information on the nature of respiratory states that makes the technical terms readily
 155 recognized and more easy to understand.

156 **Figure 1. Mitochondrial respiration**
 157 **is the oxidation of fuel substrates**
 158 **(electron donors) and reduction of**
 159 **O₂ catalysed by the electron**
 160 **transfer system, ETS:** (a)
 161 **mitochondrial catabolic**
 162 **respiration;** (b) **mitochondrial and**
 163 **non-mitochondrial catabolic O₂**
 164 **consumption;** O₂ **balance of (c) total**
 165 **cellular O₂ consumption and (d)**
 166 **external respiration**



167 All chemical reactions, r , that
 168 consume O₂ in the cells of an
 169 organism, contribute to cell
 170 respiration, J_{rO_2} . ❶ Non-mitochondrial
 171 O₂ consumption by catabolic
 172 reactions, particularly peroxisomal
 173 oxidases; ❷ mitochondrial residual
 174 oxygen consumption, Rox , after
 175 blocking the ETS; ❸ non-
 176 mitochondrial Rox ; ❹ extracellular O₂
 177 consumption; ❺ aerobic microbial
 178 respiration. Bars are not at a
 179 quantitative scale.

180 **a Mitochondrial catabolic**
 181 **respiration, J_{kO_2} , is the O₂**
 182 **consumption by the mitochondrial**
 183 **ETS maintaining the protonmotive force, Δp . J_{kO_2} excludes Rox .**

184 **b Catabolic respiration** is the O₂ consumption associated with catabolic pathways in the cell,
 185 including peroxisomal oxidation reactions (❶) in addition to mitochondrial catabolism (*
 186 The reactions k have to be defined specifically for *a* and *b*.)

187 **c Aerobic cell respiration, J_{rO_2} , takes into account internal O₂-consuming reactions, r ,**
 188 including catabolic respiration and Rox . Internal respiration of an organism includes
 189 extracellular O₂ consumption (❹) and aerobic respiration by the microbiome (❺).
 190 Respiration is distinguished from fermentation by: (1) External electron acceptors for the
 191 maintenance of redox balance, whereas fermentation is characterized by an internal electron
 192 acceptor produced in intermediary metabolism. In aerobic cell respiration, redox balance is
 193 maintained by O₂ as the electron acceptor. (2) Compartmental coupling in vectorial oxidative
 194 phosphorylation, in contrast to exclusively scalar substrate-level phosphorylation in
 195 fermentation.

196 **d External respiration** balances internal respiration at steady-state. O₂ is transported from the
 197 environment across the respiratory cascade (circulation between tissues and diffusion across
 198 cell membranes) to the intracellular compartment, while bicarbonate and CO₂ are transported
 199 in reverse to the extracellular milieu and the organismic environment. Hemoglobin provides
 200 the molecular paradigm for the combination of O₂ and CO₂ exchange, as do lungs and gills
 201 on the morphological level. The respiratory quotient, RQ , is the molar CO₂/O₂ exchange
 202 ratio; when combined with the respiratory nitrogen quotient, N/O₂ (mol N given off per mol
 203 O₂ consumed), the RQ reflects the proportion of carbohydrate, lipid and protein utilized in
 204 cell respiration during aerobically balanced steady-states.

205

- 206 4. Mitochondrial coupling states are defined according to the control of respiratory oxygen
 207 flux by the protonmotive force. Capacities of oxidative phosphorylation and
 208 electron transfer are measured at kinetically saturating concentrations of fuel
 209 substrates, ADP and inorganic phosphate, or at optimal uncoupler concentrations,
 210 respectively, in the absence of Complex IV inhibitors such as NO, CO, or H₂S.
 211 Respiratory capacity is a measure of the upper bound of the rate of respiration,
 212 depends on the substrate type undergoing oxidation, and provides reference values
 213 for the diagnosis of health and disease, and for evaluation of the effects of
 214 Evolutionary background, Age, Gender and sex, Lifestyle and Environment
 215 (EAGLE).
- 216 5. Incomplete tightness of coupling, *i.e.*, some degree of uncoupling relative to the
 217 substrate-dependent coupling stoichiometry, is a characteristic of energy-
 218 transformations across membranes. Uncoupling is caused by a variety of
 219 physiological, pathological, toxicological, pharmacological and environmental
 220 conditions that exert an influence not only on the proton leak and cation cycling,
 221 but also on proton slip within the proton pumps and the structural integrity of the
 222 mitochondria. A more loosely coupled state is induced by stimulation of
 223 mitochondrial superoxide formation and the bypass of proton pumps. In addition,
 224 uncoupling by application of protonophores represents an experimental
 225 intervention for the transition from a well-coupled to the noncoupled state of
 226 mitochondrial respiration.
- 227 6. Respiratory oxygen consumption rates have to be carefully normalized to enable meta-
 228 analytic studies beyond the specific question of a particular experiment. Therefore,
 229 all raw data should be published in a supplemental table or open access data
 230 repository. Normalization of rates for the volume of the experimental chamber (the
 231 measuring system) is distinguished from normalization for: (1) the volume or mass
 232 of the experimental sample; (2) the number of objects (cells, organisms); and (3)
 233 the concentration of mitochondrial markers in the chamber.
- 234 7. The consistent use of terms and symbols will facilitate transdisciplinary communication
 235 and support further developments of a database on bioenergetics and mitochondrial
 236 physiology. The present considerations are focused on studies with mitochondrial
 237 preparations. These will be extended in a series of reports on pathway control of
 238 mitochondrial respiration, the protonmotive force, respiratory states in intact cells,
 239 and harmonization of experimental procedures.
 240

241 **Box 1: In brief – Mitochondria and Bioblasts**

242
 243 *‘For the physiologist, mitochondria afforded the first opportunity for an
 244 experimental approach to structure-function relationships, in particular those
 245 involved in active transport, vectorial metabolism, and metabolic control
 246 mechanisms on a subcellular level’* (Ernster and Schatz 1981).
 247

248 **Mitochondria** are the oxygen-consuming electrochemical generators evolved from
 249 endosymbiotic bacteria (Margulis 1970; Lane 2005). They were described by Richard Altmann
 250 (1894) as ‘bioblasts’, which include not only the mitochondria as presently defined, but also
 251 symbiotic and free-living bacteria. The word ‘mitochondria’ (Greek mitos: thread; chondros:
 252 granule) was introduced by Carl Benda (1898).

253 Mitochondria form dynamic networks within eukaryotic cells and are morphologically
 254 enclosed by a double membrane. The mitochondrial inner membrane (mtIM) shows dynamic
 255 tubular to disk-shaped cristae that separate the mitochondrial matrix, *i.e.*, the negatively charged
 256 internal mitochondrial compartment, from the intermembrane space; the latter being enclosed
 257 by the mitochondrial outer membrane (mtOM) and positively charged with respect to the

258 matrix. The mtIM contains the non-bilayer phospholipid cardiolipin, which is not present in
259 any other eukaryotic cellular membrane. Cardiolipin stabilizes and promotes the formation of
260 respiratory supercomplexes (SC I_nIII_nIV_n), which are supramolecular assemblies based upon
261 specific, though dynamic interactions between individual respiratory complexes (Greggio *et al.*
262 2017; Lenaz *et al.* 2017). Membrane fluidity exerts an influence on functional properties of
263 proteins incorporated in the membranes (Waczulikova *et al.* 2007). In addition to mitochondrial
264 movement along microtubules, mitochondrial morphology can change in response to energy
265 requirements of the cell via processes known as fusion and fission, through which mitochondria
266 communicate within a network (Chan 2006). Intracellular stress factors may cause shrinking or
267 swelling of the mitochondrial matrix, that can ultimately result in permeability transition.

268 Mitochondria are the structural and functional elements of cell respiration. Mitochondrial
269 respiration is the reduction of molecular oxygen by electron transfer coupled to electrochemical
270 proton translocation across the mtIM. In the process of oxidative phosphorylation (OXPHOS),
271 the catabolic reaction of oxygen consumption is electrochemically coupled to the
272 transformation of energy in the form of adenosine triphosphate (ATP; Mitchell 1961, 2011).
273 Mitochondria are the powerhouses of the cell which contain the machinery of the OXPHOS-
274 pathways, including transmembrane respiratory complexes (proton pumps with FMN, Fe-S and
275 cytochrome *b*, *c*, *aa*₃ redox systems); alternative dehydrogenases and oxidases; the coenzyme
276 ubiquinone (Q); F-ATPase or ATP synthase; the enzymes of the tricarboxylic acid cycle, fatty
277 acid and amino acid oxidation; transporters of ions, metabolites and co-factors; iron/sulphur
278 cluster synthesis; and mitochondrial kinases related to energy transfer pathways. The
279 mitochondrial proteome comprises over 1,200 proteins (Calvo *et al.* 2015; 2017), mostly
280 encoded by nuclear DNA (nDNA), with a variety of functions, many of which are relatively
281 well known (*e.g.*, proteins regulating mitochondrial biogenesis or apoptosis), while others are
282 still under investigation, or need to be identified (*e.g.*, alanine transporter). Only lately it is
283 possible to use the mammalian mitochondrial proteome to discover and characterize the genetic
284 basis of mitochondrial diseases (Williams *et al.* 2016; Palmfeldt and Bross 2017).

285 There is a constant crosstalk between mitochondria and the other cellular components.
286 The crosstalk between mitochondria and endoplasmic reticulum is involved in the regulation of
287 calcium homeostasis, cell division, autophagy, differentiation, and anti-viral signaling (Murley
288 and Nunnari 2016). Mitochondria contribute to the formation of peroxisomes, which are hybrids
289 of mitochondrial and ER-derived precursors (Sugiura *et al.* 2017). Cellular mitochondrial
290 homeostasis (mitostasis) is maintained through regulation at both the transcriptional and post-
291 translational level. Cell signalling modules contribute to homeostatic regulation throughout the
292 cell cycle or even cell death by activating proteostatic modules (*e.g.*, the ubiquitin-proteasome
293 and autophagy-lysosome/vacuole pathways; specific proteases like LON) and genome stability
294 modules in response to varying energy demands and stress cues (Quiros *et al.* 2016).
295 Acetylation is a post-translational modification capable of influencing the bioenergetic
296 response, with clinically significant implications for health and disease (Carrico *et al.* 2018).
297 Mitochondria can traverse cell boundaries in a process known as horizontal mitochondrial
298 transfer (Torralba *et al.* 2016).

299 Mitochondria typically maintain several copies of their own circular genome known as
300 mitochondrial DNA (mtDNA; hundred to thousands per cell; Cummins 1998), which is
301 maternally inherited. Biparental mitochondrial inheritance is documented in mammals, birds,
302 fish, reptiles and invertebrate groups, and is even the norm in some bivalve taxonomic groups
303 (Breton *et al.* 2007; White *et al.* 2008). The mitochondrial genome of the angiosperm *Amborella*
304 contains a record of six mitochondrial genome equivalents acquired by horizontal transfer of
305 entire genomes, two from angiosperms, three from algae and one from mosses (Rice *et al.*
306 2016). However, some organisms such as *Cryptosporidium* species have morphologically and
307 functionally reduced mitochondria without DNA (Liu *et al.* 2016). In vertebrates but not all
308 invertebrates, mtDNA is compact (16.5 kB in humans) and encodes 13 protein subunits of the

309 transmembrane respiratory Complexes CI, CIII, CIV and F-ATPase, 22 tRNAs, and two RNAs.
310 Additional gene content has been suggested to include microRNAs, piRNA, smithRNAs, repeat
311 associated RNA, and even additional proteins (Duarte *et al.* 2014; Lee *et al.* 2015; Cobb *et al.*
312 2016). The mitochondrial genome requires nuclear-encoded mitochondrially targeted proteins
313 for its maintenance and expression (Rackham *et al.* 2012). Both genomes encode peptides of
314 the membrane spanning redox pumps (CI, CIII and CIV) and F-ATPase, leading to strong
315 constraints in the coevolution of both genomes (Blier *et al.* 2001).

316 Mitochondrial dysfunction is associated with a wide variety of genetic and degenerative
317 diseases. Robust mitochondrial function is supported by physical exercise and caloric balance,
318 and is central for sustained metabolic health throughout life. Therefore, a more consistent
319 presentation of mitochondrial physiology will improve our understanding of the etiology of
320 disease, the diagnostic repertoire of mitochondrial medicine, with a focus on protective
321 medicine, lifestyle and healthy aging.

322 Abbreviation: mt, as generally used in mtDNA. Mitochondrion is singular and
323 mitochondria is plural.

325 326 **1. Introduction**

327
328 Mitochondria are the powerhouses of the cell with numerous physiological, molecular,
329 and genetic functions (**Box 1**). Every study of mitochondrial health and disease is faced with
330 Evolution, Age, Gender and sex, Lifestyle, and Environment (EAGLE) as essential background
331 conditions intrinsic to the individual person or cohort, species, tissue and to some extent even
332 cell line. As a large and coordinated group of laboratories and researchers, the mission of the
333 global MitoEAGLE Network is to generate the necessary scale, type, and quality of consistent
334 data sets and conditions to address this intrinsic complexity. Harmonization of experimental
335 protocols and implementation of a quality control and data management system are required to
336 interrelate results gathered across a spectrum of studies and to generate a rigorously monitored
337 database focused on mitochondrial respiratory function. In this way, researchers from a variety
338 of disciplines can compare their findings using clearly defined and accepted international
339 standards.

340 Reliability and comparability of quantitative results depend on the accuracy of
341 measurements under strictly-defined conditions. A conceptual framework is required to warrant
342 meaningful interpretation and comparability of experimental outcomes carried out by research
343 groups at different institutes. With an emphasis on quality of research, collected data can be
344 useful far beyond the specific question of a particular experiment. Standardization and
345 homogenization of terminology, methodology, and data sets could lead to the development of
346 open-access databases such as those that have been developed for National Institutes of Health
347 sponsored research in genetics, proteomics, and metabolomics. Enabling meta-analytic studies
348 is the most economic way of providing robust answers to biological questions (Cooper *et al.*
349 2009). Vague or ambiguous jargon can lead to confusion and may relegate valuable signals to
350 wasteful noise. For this reason, measured values must be expressed in standard units for each
351 parameter used to define mitochondrial respiratory function. Harmonization of nomenclature
352 and definition of technical terms are essential to improve the awareness of the intricate meaning
353 of current and past scientific vocabulary, for documentation and integration into databases in
354 general, and quantitative modelling in particular (Beard 2005). The focus on coupling states
355 and fluxes through metabolic pathways of aerobic energy transformation in mitochondrial
356 preparations is a first step in the attempt to generate a conceptually-oriented nomenclature in
357 bioenergetics and mitochondrial physiology. Coupling states of intact cells, the protonmotive
358 force, and respiratory control by fuel substrates and specific inhibitors of respiratory enzymes
359 will be reviewed in subsequent communications.

2. Oxidative phosphorylation and coupling states in mitochondrial preparations

‘Every professional group develops its own technical jargon for talking about matters of critical concern ... People who know a word can share that idea with other members of their group, and a shared vocabulary is part of the glue that holds people together and allows them to create a shared culture’ (Miller 1991).

Mitochondrial preparations are defined as either isolated mitochondria, or tissue and cellular preparations in which the barrier function of the plasma membrane is disrupted. Since this entails the loss of cell viability, mitochondrial preparations are not studied *in vivo*. In contrast to isolated mitochondria and tissue homogenate preparations, mitochondria in permeabilized tissues and cells are *in situ* relative to the plasma membrane. The plasma membrane separates the intracellular compartment including the cytosol, nucleus, and organelles from the extracellular environment. The plasma membrane consists of a lipid bilayer with embedded proteins and attached organic molecules that collectively control the selective permeability of ions, organic molecules, and particles across the cell boundary. The intact plasma membrane prevents the passage of many water-soluble mitochondrial substrates and inorganic ions—such as succinate, adenosine diphosphate (ADP) and inorganic phosphate (P_i), that must be controlled at kinetically-saturating concentrations for the analysis of respiratory capacities. Despite of the activity of solute carriers, *e.g.*, SLC13A3 and SLC20A2, that transport these metabolites across the plasma membrane of various cell types, this limits the scope of investigations into mitochondrial respiratory function in intact cells (**Figure 2A**).

The cholesterol content of the plasma membrane is high compared to mitochondrial membranes. Therefore, mild detergents—such as digitonin and saponin—can be applied to selectively permeabilize the plasma membrane by interaction with cholesterol and allow free exchange of organic molecules and inorganic ions between the cytosol and the immediate cell environment, while maintaining the integrity and localization of organelles, cytoskeleton, and the nucleus. Application of optimum concentrations of permeabilization agents (mild detergents or toxins) leads to washout of cytosolic marker enzymes—such as lactate dehydrogenase—and results in the complete loss of cell viability, tested by nuclear staining using membrane-impermeable dyes, while mitochondrial function remains intact, tested by cytochrome *c* addition, for example. Respiration of isolated mitochondria remains unaltered after the addition of low concentrations of digitonin or saponin. In addition to mechanical cell disruption during homogenization of tissue, permeabilization agents may be applied to ensure permeabilization of all cells in tissue homogenates. Suspensions of cells permeabilized in the respiration chamber and crude tissue homogenates contain all components of the cell at highly dilute concentrations. All mitochondria are retained in chemically-permeabilized mitochondrial preparations and crude tissue homogenates. In the preparation of isolated mitochondria, however, the mitochondria are separated from other cell fractions and purified by differential centrifugation, entailing the loss of a fraction of the total mitochondrial content. Typical mitochondrial recovery ranges from 30% to 80%. Using Percoll or sucrose density gradients to maximize the purity of isolated mitochondria may compromise the mitochondrial yield or structural and functional integrity. Therefore, protocols to isolate mitochondria need to be optimized according to each study. The term mitochondrial preparation does neither include further fractionation of mitochondrial components, nor submitochondrial particles.

2.1. Respiratory control and coupling

Respiratory coupling control states are established in studies of mitochondrial preparations to obtain reference values for various output variables (**Table 1**). Physiological conditions *in vivo* deviate from these experimentally obtained states. Since kinetically-saturating concentrations, *e.g.*, of ADP or oxygen (O_2 ; dioxygen), may not apply to

411 physiological intracellular conditions, relevant information is obtained in studies of kinetic
 412 responses to variations in [ADP] or [O₂] in the range between kinetically-saturating
 413 concentrations and anoxia (Gnaiger 2001).

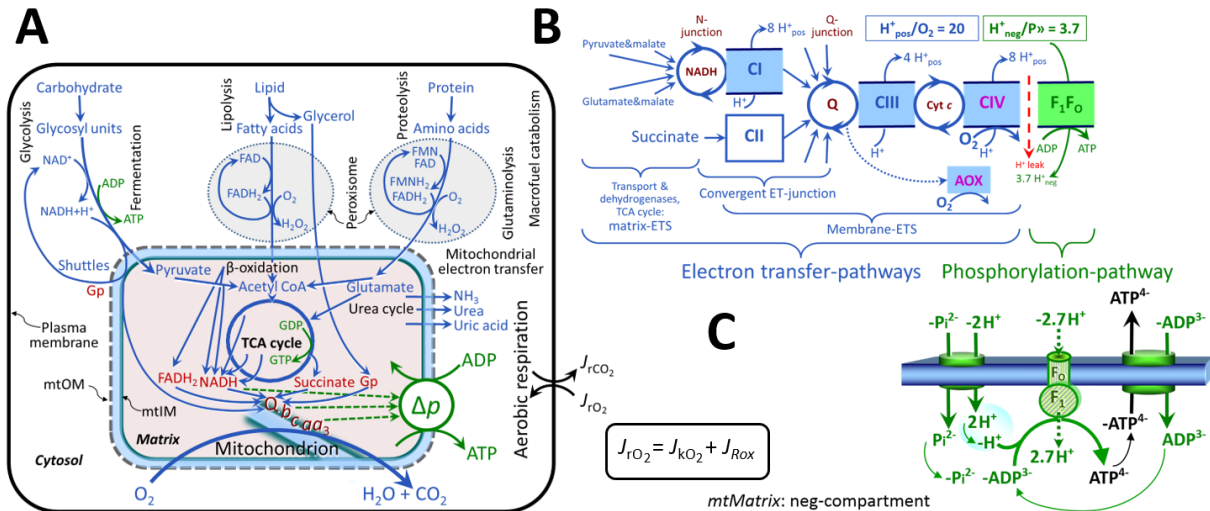
414 **The steady-state:** Mitochondria represent a thermodynamically open system in non-
 415 equilibrium states of biochemical energy transformation. State variables (protonmotive force;
 416 redox states) and metabolic *rates* (fluxes) are measured in defined mitochondrial respiratory
 417 *states*. Steady-states can be obtained only in open systems, in which changes by *internal*
 418 transformations, *e.g.*, O₂ consumption, are instantaneously compensated for by *external* fluxes,
 419 *e.g.*, O₂ supply, preventing a change of O₂ concentration in the system (Gnaiger 1993b).
 420 Mitochondrial respiratory states monitored in closed systems satisfy the criteria of pseudo-
 421 steady states for limited periods of time, when changes in the system (concentrations of O₂, fuel
 422 substrates, ADP, P_i, H⁺) do not exert significant effects on metabolic fluxes (respiration,
 423 phosphorylation). Such pseudo-steady states require respiratory media with sufficient buffering
 424 capacity and substrates maintained at kinetically-saturating concentrations, and thus depend on
 425 the kinetics of the processes under investigation.

426 **Specification of biochemical dose:** Substrates, uncouplers, inhibitors, and other
 427 chemical reagents are titrated to dissect mitochondrial function. Nominal concentrations of
 428 these substances are usually reported as initial amount of substance concentration [mol·L⁻¹] in
 429 the incubation medium. When aiming at the measurement of kinetically saturated processes—
 430 such as OXPHOS-capacities, the concentrations for substrates can be chosen according to the
 431 apparent equilibrium constant, K_m' . In the case of hyperbolic kinetics, only 80% of maximum
 432 respiratory capacity is obtained at a substrate concentration of four times the K_m' , whereas
 433 substrate concentrations of 5, 9, 19 and 49 times the K_m' are theoretically required for reaching
 434 83%, 90%, 95% or 98% of the maximal rate (Gnaiger 2001). Other reagents are chosen to
 435 inhibit or alter some processes. The amount of these chemicals in an experimental incubation
 436 is selected to maximize effect, avoiding unacceptable off-target consequences that would
 437 adversely affect the data being sought. Specifying the amount of substance in an incubation as
 438 nominal concentration in the aqueous incubation medium can be ambiguous (Doskey *et al.*
 439 2015), particularly for lipophilic substances (oligomycin, uncouplers, permeabilization agents)
 440 or cations (TPP⁺; fluorescent dyes such as safranin, TMRM; Chowdhury *et al.* 2015), which
 441 accumulate in biological membranes or in the mitochondrial matrix. For example, a dose of
 442 digitonin of 8 fmol·cell⁻¹ (10 pg·cell⁻¹; 10 µg·10⁻⁶ cells) is optimal for permeabilization of
 443 endothelial cells, and the concentration in the incubation medium has to be adjusted according
 444 to the cell density applied (Doerrier *et al.* 2018).

445 Generally, dose/exposure can be specified per unit of biological sample, *i.e.*, (nominal
 446 moles of xenobiotic)/(number of cells) [mol·cell⁻¹] or, as appropriate, per mass of biological
 447 sample [mol·kg⁻¹]. This approach to specification of dose/exposure provides a scalable
 448 parameter that can be used to design experiments, help interpret a wide variety of experimental
 449 results, and provide absolute information that allows researchers worldwide to make the most
 450 use of published data (Doskey *et al.* 2015).

451 **Phosphorylation, P_», and P_»/O₂ ratio:** *Phosphorylation* in the context of OXPHOS is
 452 defined as phosphorylation of ADP by P_i to form ATP. On the other hand, the term
 453 phosphorylation is used generally in many contexts, *e.g.*, protein phosphorylation. This justifies
 454 consideration of a symbol more discriminating and specific than P as used in the P/O ratio
 455 (phosphate to atomic oxygen ratio), where P indicates phosphorylation of ADP to ATP or GDP
 456 to GTP (**Figure 2**). We propose the symbol P_» for the endergonic (uphill) direction of
 457 phosphorylation ADP→ATP, and likewise the symbol P_« for the corresponding exergonic
 458 (downhill) hydrolysis ATP→ADP (**Figure 3**). P_» refers mainly to electrontransfer
 459 phosphorylation but may also involve substrate-level phosphorylation as part of the
 460 tricarboxylic acid (TCA) cycle (succinyl-CoA ligase; phosphoglycerate kinase) and
 461 phosphorylation of ADP catalyzed by pyruvate kinase, and of GDP phosphorylated by

462 phosphoenolpyruvate carboxykinase. Transphosphorylation is performed by adenylate kinase,
 463 creatine kinase (mtCK), hexokinase and nucleoside diphosphate kinase. In isolated mammalian
 464 mitochondria, ATP production catalyzed by adenylate kinase ($2 \text{ ADP} \leftrightarrow \text{ATP} + \text{AMP}$) proceeds
 465 without fuel substrates in the presence of ADP (Komlódi and Tretter 2017). Kinase cycles are
 466 involved in intracellular energy transfer and signal transduction for regulation of energy flux.
 467



468

469

Figure 2. Cell respiration and oxidative phosphorylation (OXPHOS)

470

Mitochondrial respiration is the oxidation of fuel substrates (electron donors) with electron transfer to O₂ as the electron acceptor. For explanation of symbols see also **Figure 1**.

471

472

(A) Respiration of intact cells: Extra-mitochondrial catabolism of macrofuels or uptake of small molecules by the cell provides the *mitochondrial* fuel substrates. Many fuel substrates are catabolized to acetyl-CoA or to glutamate, and further electron transfer reduces nicotinamide adenine dinucleotide to NADH or flavin adenine dinucleotide to FADH₂. In aerobic respiration, electron transfer is coupled to the phosphorylation of ADP to ATP, with energy transformation mediated by the protonmotive force, Δp. Anabolic reactions are linked to catabolism, both by ATP as the intermediary energy currency and by small organic precursor molecules as building blocks for biosynthesis (not shown). Glycolysis involves substrate-level phosphorylation of ADP to ATP in fermentation without utilization of O₂. In contrast, extra-mitochondrial oxidation of fatty acids and amino acids proceeds partially in peroxisomes without coupling to ATP production: acyl-CoA oxidase catalyzes the oxidation of FADH₂ with electron transfer to O₂; amino acid oxidases oxidize flavin mononucleotide FMNH₂ or FADH₂. Coenzyme Q, Q, and the cytochromes *b*, *c*, and *aa*₃ are redox systems of the mitochondrial inner membrane, mtIM. Dashed arrows indicate the connection between the redox proton pumps (respiratory Complexes CI, CIII and CIV) and the transmembrane Δp. Mitochondrial outer membrane, mtOM; glycerol-3-phosphate, Gp; tricarboxylic acid cycle, TCA cycle.

473

474

475

476

477

478

479

480

481

482

483

484

485

486

487

488

489

(B) Respiration in mitochondrial preparations: The mitochondrial electron transfer system (ETS) is (1) fuelled by diffusion and transport of substrates across the mitochondrial outer and inner membrane, and in addition consists of the (2) matrix-ETS, and (3) membrane-ETS. Upstream sections of ET-pathways converge at the N-junction and Q-junction. Unspecified arrows converging at the Q-junction indicate additional upstream ET-sections with electron entry through electron transferring flavoprotein, glycerophosphate dehydrogenase, dihydroorotate dehydrogenase, choline dehydrogenase, and sulfide-ubiquinone oxidoreductase. The dotted arrow indicates the branched pathway of oxygen consumption by alternative quinol oxidase (AOX). ET-pathways are coupled to the phosphorylation-pathway. The H⁺_{pos}/O₂ ratio is the outward proton flux from the matrix space to the positively (pos) charged vesicular compartment, divided by catabolic O₂ flux in the NADH-pathway. The H⁺_{neg}/P ratio is the inward proton flux from the inter-membrane space to the negatively (neg) charged matrix space,

499

500 divided by the flux of phosphorylation of ADP to ATP. These stoichiometries are not fixed due
501 to ion leaks and proton slip.

502 (C) Chemiosmotic phosphorylation-pathway catalyzed by the proton pump F₁F₀-ATPase (F-
503 ATPase, ATP synthase), adenine nucleotide translocase, and inorganic phosphate transporter.
504 The H⁺_{neg}/P_» stoichiometry is the sum of the coupling stoichiometry in the F-ATPase reaction
505 (-2.7 H⁺_{pos} from the positive intermembrane space, 2.7 H⁺_{neg} to the matrix, *i.e.*, the negative
506 compartment) and the proton balance in the translocation of ADP³⁻, ATP⁴⁻ and P_i²⁻. Modified
507 from (B) Lemieux *et al.* (2017) and (C) Gnaiger (2014).

508

509 The P_»/O₂ ratio (P_»/4 e⁻) is two times the ‘P/O’ ratio (P_»/2 e⁻) of classical bioenergetics.
510 P_»/O₂ is a generalized symbol, not specific for determination of P_i consumption (P_i/O₂ flux
511 ratio), ADP depletion (ADP/O₂ flux ratio), or ATP production (ATP/O₂ flux ratio). The
512 mechanistic P_»/O₂ ratio—or P_»/O₂ stoichiometry—is calculated from the proton-to-O₂ and
513 proton-to-phosphorylation coupling stoichiometries (**Figure 2B**):
514

$$515 \quad P_{\gg}/O_2 = \frac{H_{\text{pos}}^+/O_2}{H_{\text{neg}}^+/P_{\gg}} \quad (1)$$

516

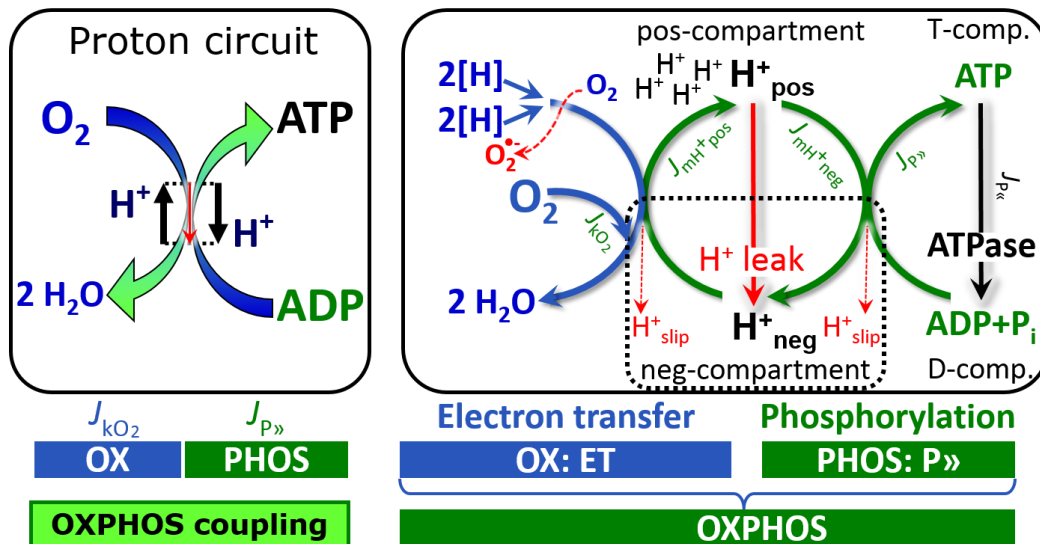
517 The H⁺_{pos}/O₂ *coupling stoichiometry* (referring to the full 4 electron reduction of O₂) depends
518 on the relative involvement of the three coupling sites (respiratory Complexes I, III and IV; CI,
519 CIII and CIV) in the catabolic ET-pathway from reduced fuel substrates (electron donors) to
520 the reduction of O₂ (electron acceptor). This varies with: (1) a bypass of CI by single or multiple
521 electron input into the Q-junction; and (2) a bypass of CIV by involvement of alternative
522 oxidases, AOX, which are not expressed in mammalian mitochondria.

523 H⁺_{pos}/O₂ is 12 in the ET-pathways involving CIII and CIV as proton pumps, increasing to
524 20 for the NADH-pathway through CI (**Figure 2B**), but a general consensus on H⁺_{pos}/O₂
525 stoichiometries remains to be reached (Hinkle 2005; Wikström and Hummer 2012; Sazanov
526 2015). The H⁺_{neg}/P_» coupling stoichiometry (3.7; **Figure 2B**) is the sum of 2.7 H⁺_{neg} required
527 by the F-ATPase of vertebrate and most invertebrate species (Watt *et al.* 2010) and the proton
528 balance in the translocation of ADP, ATP and P_i (**Figure 2C**). Taken together, the mechanistic
529 P_»/O₂ ratio is calculated at 5.4 and 3.3 for NADH- and succinate-linked respiration, respectively
530 (Eq. 1). The corresponding classical P_»/O ratios (referring to the 2 electron reduction of 0.5 O₂)
531 are 2.7 and 1.6 (Watt *et al.* 2010), in agreement with the measured P_»/O ratio for succinate of
532 1.58 ± 0.02 (Gnaiger *et al.* 2000).

533 The effective P_»/O₂ flux ratio ($Y_{P_{\gg}/O_2} = J_{P_{\gg}}/J_{kO_2}$; **Figure 3**) is diminished relative to the
534 mechanistic P_»/O₂ ratio by intrinsic and extrinsic uncoupling and dyscoupling (**Figure 4**). Such
535 generalized uncoupling is different from switching to mitochondrial pathways that involve
536 fewer than three proton pumps (‘coupling sites’: Complexes CI, CIII and CIV), bypassing CI
537 through multiple electron entries into the Q-junction, or CIII and CIV through AOX (**Figure**
538 **2B**). Reprogramming of mitochondrial pathways leading to different types of substrates being
539 oxidized may be considered as a switch of gears (changing the stoichiometry by altering the
540 substrate that is oxidized) rather than uncoupling (loosening the tightness of coupling relative
541 to a fixed stoichiometry). In addition, Y_{P_{\gg}/O_2} depends on several experimental conditions of flux
542 control, increasing as a hyperbolic function of [ADP] to a maximum value (Gnaiger 2001).

543 **Control and regulation:** The terms metabolic *control* and *regulation* are frequently used
544 synonymously, but are distinguished in metabolic control analysis: ‘We could understand the
545 regulation as the mechanism that occurs when a system maintains some variable constant over
546 time, in spite of fluctuations in external conditions (homeostasis of the internal state). On the
547 other hand, metabolic control is the power to change the state of the metabolism in response to
548 an external signal’ (Fell 1997). Respiratory control may be induced by experimental control
549 signals that *exert* an influence on: (1) ATP demand and ADP phosphorylation-rate; (2) fuel
550 substrate composition, pathway competition; (3) available amounts of substrates and O₂, *e.g.*,

551 starvation and hypoxia; (4) the protonmotive force, redox states, flux–force relationships,
 552 coupling and efficiency; (5) Ca^{2+} and other ions including H^+ ; (6) inhibitors, *e.g.*, nitric oxide
 553 or intermediary metabolites such as oxaloacetate; (7) signalling pathways and regulatory
 554 proteins, *e.g.*, insulin resistance, transcription factor hypoxia inducible factor 1. *Mechanisms* of
 555 respiratory control and regulation include adjustments of: (1) enzyme activities by allosteric
 556 mechanisms and phosphorylation; (2) enzyme content, concentrations of cofactors and
 557 conserved moieties—such as adenylates, nicotinamide adenine dinucleotide [NAD^+/NADH],
 558 coenzyme Q, cytochrome *c*; (3) metabolic channeling by supercomplexes; and (4)
 559 mitochondrial density (enzyme concentrations and membrane area) and morphology (cristae
 560 folding, fission and fusion). Mitochondria are targeted directly by hormones, thereby affecting
 561 their energy metabolism (Lee *et al.* 2013; Gerö and Szabo 2016; Price and Dai 2016; Moreno
 562 *et al.* 2017). Evolutionary or acquired differences in the genetic and epigenetic basis of
 563 mitochondrial function (or dysfunction) between individuals; age; gender, biological sex, and
 564 hormone concentrations; life style including exercise and nutrition; and environmental issues
 565 including thermal, atmospheric, toxic and pharmacological factors, exert an influence on all
 566 control mechanisms listed above. For reviews, see Brown 1992; Gnaiger 1993a, 2009; 2014;
 567 Paradies *et al.* 2014; Morrow *et al.* 2017.
 568



569 **Figure 3. Coupling in oxidative phosphorylation (OXPHOS)**

570 $2[\text{H}]$ indicates the reduced hydrogen equivalents of fuel substrates of the catabolic reaction *k*
 571 with oxygen. O_2 flux, J_{kO_2} , through the catabolic ET-pathway, is coupled to flux through the
 572 phosphorylation-pathway of ADP to ATP, $J_{\text{P}\gg}$. The redox proton pumps of the ET-pathway
 573 drive proton flux into the positive (pos) compartment, $J_{\text{mH}^+\text{pos}}$, generating the output
 574 protonmotive force (motive, subscript *m*). F-ATPase is coupled to inward proton current into
 575 the negative (neg) compartment, $J_{\text{mH}^+\text{neg}}$, to phosphorylate ADP to ATP. The system is defined
 576 by the boundaries (full black line) and is not a black box, but is analysed as a compartmental
 577 system. The negative compartment (neg-compartment, enclosed by the dotted line) is the
 578 matrix space, separated by the mtIM from the positive compartment (pos-compartment).
 579 $\text{ADP}+\text{P}_i$ and ATP are the substrate- and product-compartments (scalar ADP and ATP
 580 compartments, D-comp. and T-comp.), respectively. At steady-state proton turnover, $J_{\infty\text{H}^+}$, and
 581 ATP turnover, $J_{\infty\text{P}}$, maintain concentrations constant, when $J_{\text{mH}^+\infty} = J_{\text{mH}^+\text{pos}} = J_{\text{mH}^+\text{neg}}$, and $J_{\text{P}\gg} = J_{\text{P}\ll} = J_{\text{P}\infty}$. Modified from Gnaiger (2014).
 582
 583

584 **Respiratory control and response:** Lack of control by a metabolic pathway, *e.g.*,
 585 phosphorylation-pathway, means that there will be no response to a variable activating it, *e.g.*,
 586 $[\text{ADP}]$. The reverse, however, is not true as the absence of a response to $[\text{ADP}]$ does not exclude

587 the phosphorylation-pathway from having some degree of control. The degree of control of a
 588 component of the OXPHOS-pathway on an output variable—such as O₂ flux, will in general
 589 be different from the degree of control on other outputs—such as phosphorylation-flux or
 590 proton leak flux. Therefore, it is necessary to be specific as to which input and output are under
 591 consideration (Fell 1997).

592 **Respiratory coupling control and ET-pathway control:** Respiratory control refers to
 593 the ability of mitochondria to adjust O₂ flux in response to external control signals by engaging
 594 various mechanisms of control and regulation. Respiratory control is monitored in a
 595 mitochondrial preparation under conditions defined as respiratory states. When
 596 phosphorylation of ADP to ATP is stimulated or depressed, an increase or decrease is observed
 597 in electron transfer measured as O₂ flux in respiratory coupling states of intact mitochondria
 598 (‘controlled states’ in the classical terminology of bioenergetics). Alternatively, coupling of
 599 electron transfer with phosphorylation is disengaged by uncouplers. These protonophores are
 600 weak lipid-soluble acids which disrupt the barrier function of the mtIM and thus shortcircuit
 601 the protonmotive system, functioning like a clutch in a mechanical system. The corresponding
 602 coupling control state is characterized by a high O₂ flux without control by P» (noncoupled or
 603 ‘uncontrolled state’).

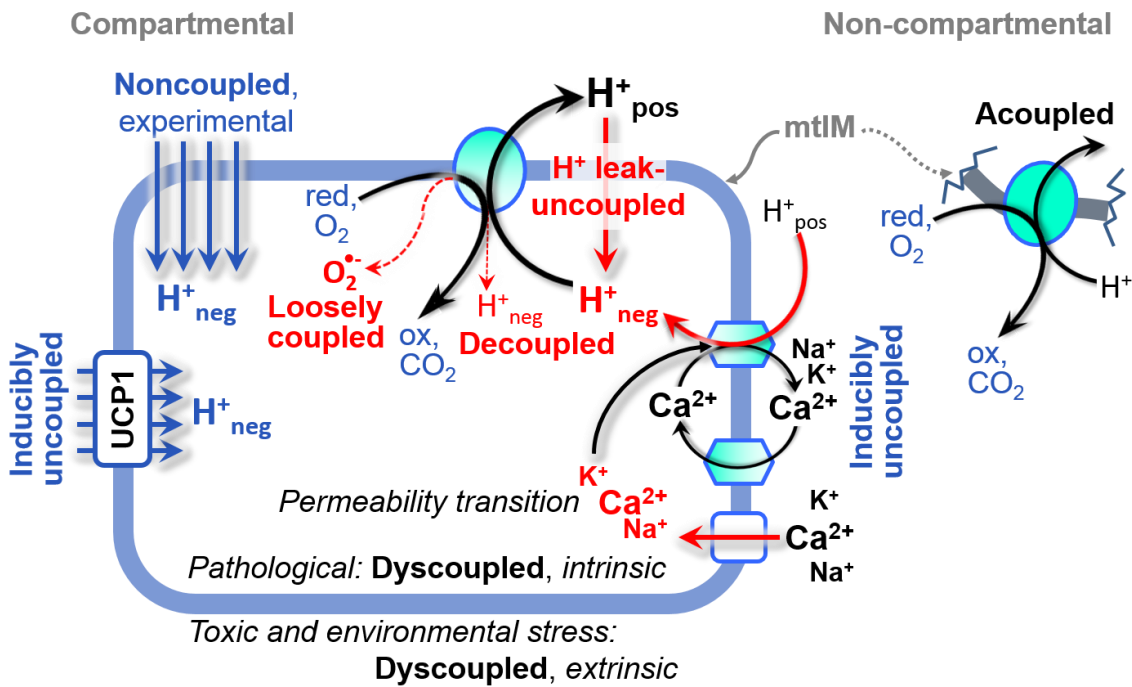
604 ET-pathway control states are obtained in mitochondrial preparations by depletion of
 605 endogenous substrates and addition to the mitochondrial respiration medium of fuel substrates
 606 (Figure 2; 2[H] in Figure 3) and specific inhibitors, activating selected mitochondrial catabolic
 607 pathways, k, of electron transfer from the oxidation of fuel substrates to reduction of O₂ (Figure
 608 2A). Coupling control states and pathway control states are complementary, since
 609 mitochondrial preparations depend on an exogenous supply of pathway-specific fuel substrates
 610 and oxygen (Gnaiger 2014).

611 **Coupling:** In mitochondrial electron transfer, vectorial transmembrane proton flux is
 612 coupled through the redox proton pumps CI, CIII and CIV to the catabolic flux of scalar
 613 reactions, collectively measured as O₂ flux (Figure 3). Thus mitochondria are elements of
 614 energy transformation. Energy is a conserved quantity and cannot be lost or produced in any
 615 internal process (First Law of thermodynamics). Open and closed systems can gain or lose
 616 energy only by external fluxes—by exchange with the environment. Therefore, energy can
 617 neither be produced by mitochondria, nor is there any internal process without energy
 618 conservation. Exergy or Gibbs energy (‘free energy’) is the part of energy that can potentially
 619 be transformed into work under conditions of constant volume and pressure. *Coupling* is the
 620 interaction of an exergonic process (spontaneous, negative exergy change) with an endergonic
 621 process (positive exergy change) in energy transformations which conserve part of the exergy
 622 that would be irreversibly lost or dissipated in an uncoupled process.

623 **Uncoupling:** Uncoupling of mitochondrial respiration is a general term comprising
 624 diverse mechanisms:

- 625 1. Proton leak across the mtIM from the pos- to the neg-compartment (H⁺ leak-
 626 uncoupled; Figure 4).
- 627 2. Cycling of other cations, strongly stimulated by permeability transition; comparable
 628 to the use of protonophores, cation cycling is experimentally induced by valinomycin
 629 in the presence of K⁺;
- 630 3. Decoupling by proton slip in the redox proton pumps when protons are effectively not
 631 pumped (CI, CIII and CIV) or are not driving phosphorylation (F-ATPase);
- 632 4. Loss of vesicular (compartmental) integrity when electron transfer is acoupled;
- 633 5. Electron leak in the loosely coupled univalent reduction of O₂ to superoxide (O₂^{•-};
 634 superoxide anion radical).

635 Differences of terms—uncoupled vs. noncoupled—are easily overlooked, although they relate
 636 to different meanings of uncoupling (Figure 4 and Table 2).



637
638
639
640
641
642
643
644
645
646
647
648
649

Figure 4. Mechanisms of respiratory uncoupling

An intact mitochondrial inner membrane, mtIM, is required for vectorial, compartmental coupling. ‘Acoupled’ respiration is the consequence of structural disruption with catalytic activity of non-compartmental mitochondrial fragments. Inducibly uncoupled (activation of UCP1) and experimentally noncoupled respiration (titration of protonophores) stimulate respiration to maximum O₂ flux. H⁺ leak-uncoupled, decoupled, and loosely coupled respiration are components of intrinsic uncoupling. Pathological dysfunction may affect all types of uncoupling, including permeability transition, causing intrinsically dyscoupled respiration. Similarly, toxicological and environmental stress factors can cause extrinsically dyscoupled respiration.

2.2. Coupling states and respiratory rates

650
651
652
653
654
655
656
657
658
659
660
661
662
663
664
665
666
667
668
669

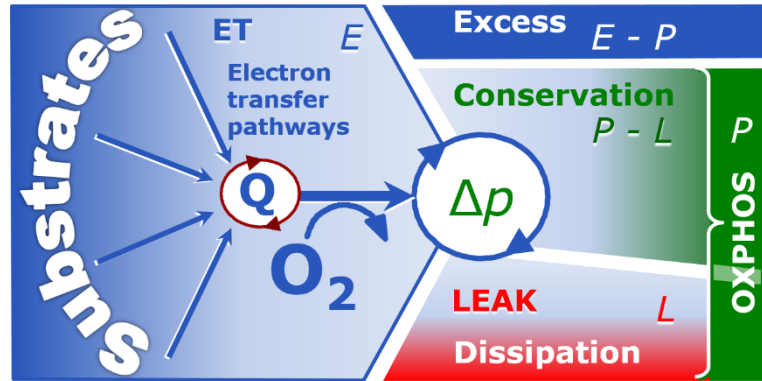
Respiratory capacities in coupling control states: To extend the classical nomenclature on mitochondrial coupling states (Section 2.3) by a concept-driven terminology that explicitly incorporates information on the meaning of respiratory states, the terminology must be general and not restricted to any particular experimental protocol or mitochondrial preparation (Gnaiger 2009). Concept-driven nomenclature aims at mapping the *meaning and concept behind* the words and acronyms onto the *forms* of words and acronyms (Miller 1991). The focus of concept-driven nomenclature is primarily the conceptual ‘why’, along with clarification of the experimental ‘how’. Respiratory capacities delineate, comparable to channel capacity in information theory (Schneider 2006), the upper bound of the rate of respiration measured in defined coupling control states and electron transfer-pathway (ET-pathway) states (Figure 5).

To provide a diagnostic reference for respiratory capacities of core energy metabolism, the capacity of *oxidative phosphorylation*, OXPHOS, is measured at kinetically-saturating concentrations of ADP and P_i. The *oxidative ET-capacity* reveals the limitation of OXPHOS-capacity mediated by the *phosphorylation-pathway*. The ET- and phosphorylation-pathways comprise coupled segments of the OXPHOS-system. ET-capacity is measured as noncoupled respiration by application of *external uncouplers*. The contribution of *intrinsically uncoupled* O₂ consumption is studied by preventing the stimulation of phosphorylation either in the absence of ADP or by inhibition of the phosphorylation-pathway. The corresponding states are collectively classified as LEAK-states, when O₂ consumption compensates mainly for ion

670 leaks, including the proton leak. Defined coupling states are induced by: (1) adding cation
 671 chelators such as EGTA, binding free Ca^{2+} and thus limiting cation cycling; (2) adding ADP
 672 and P_i ; (3) inhibiting the phosphorylation-pathway; and (4) uncoupler titrations, while
 673 maintaining a defined ET-pathway state with constant fuel substrates and inhibitors of specific
 674 branches of the ET-pathway (**Figure 5**).

675
 676 **Figure 5. Four-compartment model of oxidative phosphorylation**

677 Respiratory states (ET, OXPHOS, LEAK; **Table 1**) and corresponding rates (E , P , L) are
 678 connected by the protonmotive force, Δp . ET-capacity, E (I), is
 682 partitioned into (2) dissipative LEAK-respiration, L , when the
 685 Gibbs energy change of catabolic



687 O_2 flux is irreversibly lost, (3) net OXPHOS-capacity, $P-L$, with partial conservation of the
 688 capacity to perform work, and (4) the excess capacity, $E-P$. Modified from Gnaiger (2014).

689
 690 **Table 1. Coupling states and residual oxygen consumption in mitochondrial**
 691 **preparations in relation to respiration- and phosphorylation-flux, J_{KO_2} and J_{P} ,**
 692 **and protonmotive force, Δp .** Coupling states are established at kinetically-
 693 saturating concentrations of fuel substrates and O_2 .

State	J_{KO_2}	J_{P}	Δp	Inducing factors	Limiting factors
LEAK	L ; low, cation leak-dependent respiration	0	max.	back-flux of cations including proton leak, proton slip	$J_{\text{P}} = 0$: (1) without ADP, L_N ; (2) max. ATP/ADP ratio, L_T ; or (3) inhibition of the phosphorylation-pathway, L_{Omy}
OXPHOS	P ; high, ADP-stimulated respiration	max.	high	kinetically-saturating [ADP] and [P_i]	J_{P} , by phosphorylation-pathway; or J_{KO_2} by ET-capacity
ET	E ; max., noncoupled respiration	0	low	optimal external uncoupler concentration for max. $J_{\text{O}_2, E}$	J_{KO_2} by ET-capacity
ROX	R_{ox} ; min., residual O_2 consumption	0	0	$J_{\text{O}_2, R_{\text{ox}}}$ in non-ET-pathway oxidation reactions	inhibition of all ET-pathways; or absence of fuel substrates

694
 695 The three coupling states, ET, LEAK and OXPHOS, are shown schematically with the
 696 corresponding respiratory rates, abbreviated as E , L and P , respectively (**Figure 5**). We
 697 distinguish metabolic *pathways* from metabolic *states* and the corresponding metabolic *rates*;
 698 for example: ET-pathways, ET-states, and ET-capacities, E , respectively (**Table 1**). The
 699 protonmotive force is *high* in the OXPHOS-state when it drives phosphorylation, *maximum* in

700 the LEAK-state of coupled
701 mitochondria, driven by LEAK-
702 respiration at a minimum back-
703 flux of cations to the matrix side,
704 and *very low* in the ET-state
705 when uncouplers short-circuit the
706 proton cycle (**Table 1**).

707 **LEAK-state (Figure 6A):**

708 The LEAK-state is defined as a
709 state of mitochondrial respiration
710 when O_2 flux mainly
711 compensates for ion leaks in the
712 absence of ATP synthesis, at
713 kinetically-saturating
714 concentrations of O_2 and
715 respiratory fuel substrates.
716 LEAK-respiration is measured to
717 obtain an estimate of *intrinsic*
718 *uncoupling* without addition of
719 an experimental uncoupler: (1)
720 in the absence of adenylates, *i.e.*,
721 AMP, ADP and ATP; (2) after
722 depletion of ADP at a maximum
723 ATP/ADP ratio; or (3) after
724 inhibition of the
725 phosphorylation-pathway by
726 inhibitors of F-ATPase—such as
727 oligomycin, or of adenine
728 nucleotide translocase—such as
729 carboxyatractyloside.

730 Adjustment of the nominal
731 concentration of these inhibitors
732 to the density of biological
733 sample applied can minimize or
734 avoid inhibitory side-effects
735 exerted on ET-capacity or even
736 some dyscoupling.

737 **Proton leak and**
738 **uncoupled respiration:** Proton
739 leak is a leak current of protons.
740 The intrinsic proton leak is the
741 *uncoupled* process in which
742 protons diffuse across the mtIM
743 in the dissipative direction of the
744 downhill protonmotive force
745 without coupling to
746 phosphorylation (**Figure 6A**).

747 The proton leak flux depends non-linearly on the protonmotive force (Garlid *et al.* 1989;
748 Divakaruni and Brand 2011), it is a property of the mtIM and may be enhanced due to possible
749 contaminations by free fatty acids. Inducible uncoupling mediated by uncoupling protein 1
750 (UCP1) is physiologically controlled, *e.g.*, in brown adipose tissue. UCP1 is a member of the

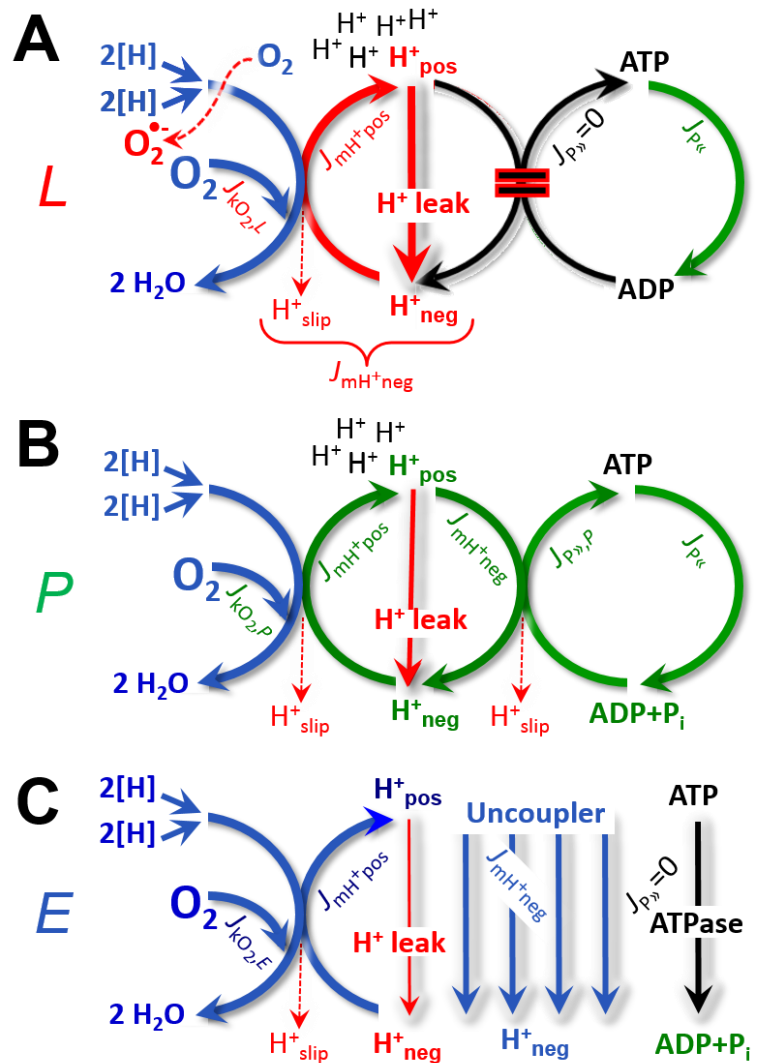


Figure 6. Respiratory coupling states

(A) **LEAK-state and rate, L :** Phosphorylation is arrested, $J_{P\gg} = 0$, and catabolic O_2 flux, $J_{kO_2,L}$, is controlled mainly by the proton leak, $J_{mH^+neg,L}$, at maximum protonmotive force (**Figure 4**). Extramitochondrial ATP may be hydrolyzed by extramitochondrial ATPases, $J_{P\ll}$.

(B) **OXPHOS-state and rate, P :** Phosphorylation, $J_{P\gg}$, is stimulated by kinetically-saturating $[ADP]$ and $[P_i]$, and is supported by a high protonmotive force. O_2 flux, $J_{kO_2,P}$, is well-coupled at a $P\gg/O_2$ ratio of $J_{P\gg,P}/J_{kO_2,P}$. Extramitochondrial ATPases may recycle ATP, $J_{P\ll}$.

(C) **ET-state and rate, E :** Noncoupled respiration, $J_{kO_2,E}$, is maximum at optimum exogenous uncoupler concentration and phosphorylation is zero, $J_{P\gg} = 0$. The F-ATPase may hydrolyze extramitochondrial ATP. See also **Figure 3**.

751 mitochondrial carrier family that is involved in the translocation of protons across the mtIM
 752 (Klingenberg 2017). Consequently, the short-circuit diminishes the protonmotive force and
 753 stimulates electron transfer to O₂ and heat dissipation without phosphorylation of ADP.

754 **Cation cycling:** There can be other cation contributors to leak current including calcium
 755 and probably magnesium. Calcium influx is balanced by mitochondrial Na⁺/Ca²⁺ or H⁺/Ca²⁺
 756 exchange, which is balanced by Na⁺/H⁺ or K⁺/H⁺ exchanges. This is another effective
 757 uncoupling mechanism different from proton leak (**Table 2**).

758
 759

Table 2. Terms on respiratory coupling and uncoupling.

Term	J_{KO_2}	$P \gg O_2$	Note	
acoupled		0	electron transfer in mitochondrial fragments without vectorial proton translocation (Figure 4)	
intrinsic, no protonophore added	uncoupled	L	0	non-phosphorylating LEAK-respiration (Figure 6A)
	proton leak-uncoupled		0	component of L , H ⁺ diffusion across the mtIM (Figure 4)
	decoupled		0	component of L , proton slip (Figure 4)
	loosely coupled		0	component of L , lower coupling due to superoxide formation and bypass of proton pumps (Figure 4)
	dyscoupled		0	pathologically, toxicologically, environmentally increased uncoupling, mitochondrial dysfunction
	inducibly uncoupled		0	by UCP1 or cation (<i>e.g.</i> , Ca ²⁺) cycling (Figure 4)
noncoupled	E	0	non-phosphorylating respiration stimulated to maximum flux at optimum exogenous uncoupler concentration (Figure 6C)	
well-coupled	P	high	phosphorylating respiration with an intrinsic LEAK component (Figure 6B)	
fully coupled	$P - L$	max.	OXPHOS-capacity corrected for LEAK-respiration (Figure 5)	

760

761 **Proton slip and decoupled respiration:** Proton slip is the *decoupled* process in which
 762 protons are only partially translocated by a redox proton pump of the ET-pathways and slip
 763 back to the original vesicular compartment. The proton leak is the dominant contributor to the
 764 overall leak current in mammalian mitochondria incubated under physiological conditions at
 765 37 °C, whereas proton slip is increased at lower experimental temperature (Canton *et al.* 1995).
 766 Proton slip can also happen in association with the F-ATPase, in which the proton slips downhill
 767 across the pump to the matrix without contributing to ATP synthesis. In each case, proton slip
 768 is a property of the proton pump and increases with the pump turnover rate.

769 **Electron leak and loosely coupled respiration:** Superoxide production by the ETS leads
 770 to a bypass of redox proton pumps and correspondingly lower $P \gg O_2$ ratio. This depends on the
 771 actual site of electron leak and the scavenging of hydrogen peroxide by cytochrome *c*, whereby
 772 electrons may re-enter the ETS with proton translocation by CIV.

773 **Loss of compartmental integrity and acoupled respiration:** Electron transfer and
 774 catabolic O₂ flux proceed without compartmental proton translocation in disrupted
 775 mitochondrial fragments. Such fragments form during mitochondrial isolation, and may not
 776 fully fuse to re-establish structurally intact mitochondria. Loss of mtIM integrity, therefore, is

777 the cause of acoupled respiration, which is a nonvectorial dissipative process without control
778 by the protonmotive force.

779 **Dyscoupled respiration:** Mitochondrial injuries may lead to *dyscoupling* as a
780 pathological or toxicological cause of *uncoupled* respiration. Dyscoupling may involve any
781 type of uncoupling mechanism, *e.g.*, opening the permeability transition pore. Dyscoupled
782 respiration is distinguished from the experimentally induced *noncoupled* respiration in the ET-
783 state (**Table 2**).

784 **OXPHOS-state (Figure 6B):** The OXPHOS-state is defined as the respiratory state with
785 kinetically-saturating concentrations of O₂, respiratory and phosphorylation substrates, and
786 absence of exogenous uncoupler, which provides an estimate of the maximal respiratory
787 capacity in the OXPHOS-state for any given ET-pathway state. Respiratory capacities at
788 kinetically-saturating substrate concentrations provide reference values or upper limits of
789 performance, aiming at the generation of data sets for comparative purposes. Physiological
790 activities and effects of substrate kinetics can be evaluated relative to the OXPHOS-capacity.

791 As discussed previously, 0.2 mM ADP does not fully saturate flux in isolated
792 mitochondria (Gnaiger 2001; Puchowicz *et al.* 2004); greater ADP concentration is required,
793 particularly in permeabilized muscle fibres and cardiomyocytes, to overcome limitations by
794 intracellular diffusion and by the reduced conductance of the mtOM (Jepihhina *et al.* 2011,
795 Illaste *et al.* 2012, Simson *et al.* 2016), either through interaction with tubulin (Rostovtseva *et al.*
796 2008) or other intracellular structures (Birkedal *et al.* 2014). In addition, saturating ADP
797 concentrations need to be evaluated under different experimental conditions such as
798 temperature (Lemieux *et al.* 2017) and with different animal models (Blier and Guderley, 1993).
799 In permeabilized muscle fibre bundles of high respiratory capacity, the apparent K_m for ADP
800 increases up to 0.5 mM (Saks *et al.* 1998), consistent with experimental evidence that >90%
801 saturation is reached only at >5 mM ADP (Pesta and Gnaiger 2012). Similar ADP
802 concentrations are also required for accurate determination of OXPHOS-capacity in human
803 clinical cancer samples and permeabilized cells (Klepinin *et al.* 2016; Koit *et al.* 2017).
804 Whereas 2.5 to 5 mM ADP is sufficient to obtain the actual OXPHOS-capacity in many types
805 of permeabilized tissue and cell preparations, experimental validation is required in each
806 specific case.

807 **Electron transfer-state (Figure 6C):** O₂ flux determined in the ET-state yields an
808 estimate of ET-capacity. The ET-state is defined as the *noncoupled* state with kinetically-
809 saturating concentrations of O₂, respiratory substrate and optimum *exogenous* uncoupler
810 concentration for maximum O₂ flux. As a consequence of the nearly collapsed protonmotive
811 force, the driving force is insufficient for phosphorylation, and $J_{P\gg} = 0$. The most frequently
812 used uncouplers are carbonyl cyanide *m*-chloro phenyl hydrazone, carbonyl cyanide *p*-
813 trifluoromethoxyphenylhydrazone or dinitrophenol (CCCP, FCCP, DNP). Stepwise titration
814 of uncouplers stimulates respiration up to or above the level of O₂ consumption rates in the
815 OXPHOS-state, but inhibition of respiration is observed above optimum uncoupler
816 concentrations (Mitchell 2011). Data obtained with a single dose of uncoupler must be
817 evaluated with caution, particularly when a fixed uncoupler concentration is used in studies
818 exploring a treatment or disease that may alter the mitochondrial content or mitochondrial
819 sensitivity to inhibition by uncouplers. The effect on ET-capacity of the reversed function of F-
820 ATPase ($J_{P\ll}$; **Figure 6C**) can be evaluated in the presence and absence of extramitochondrial
821 ATP.

822 **ROX state and *Rox*:** Besides the three fundamental coupling states of mitochondrial
823 preparations, the state of residual O₂ consumption, ROX, is relevant to assess respiratory
824 function (**Figure 1**). ROX is not a coupling state. The rate of residual oxygen consumption,
825 *Rox*, is defined as O₂ consumption due to oxidative reactions measured after inhibition of ET—
826 with rotenone, malonic acid and antimycin A. Cyanide and azide inhibit not only CIV but
827 catalase and several peroxidases involved in *Rox*. However, high concentrations of antimycin

828 A, but not rotenone or cyanide, inhibit peroxisomal acyl-CoA oxidase and D-amino acid
 829 oxidase (Vamecq *et al.* 1987). ROX represents a baseline that is used to correct respiration
 830 measured in defined coupling states. *Rox*-corrected *L*, *P* and *E* not only lower the values of total
 831 fluxes, but also changes the flux control ratios *L/P* and *L/E*. *Rox* is not necessarily equivalent
 832 to non-mitochondrial reduction of O₂, considering O₂-consuming reactions in mitochondria that
 833 are not related to ET—such as O₂ consumption in reactions catalyzed by monoamine oxidases
 834 (type A and B), monooxygenases (cytochrome P450 monooxygenases), dioxygenase (sulfur
 835 dioxygenase and trimethyllysine dioxygenase), and several hydroxylases. Even isolated
 836 mitochondrial fractions, especially those obtained from liver, may be contaminated by
 837 peroxisomes. This fact makes the exact determination of mitochondrial O₂ consumption and
 838 mitochondria-associated generation of reactive oxygen species complicated (Schönfeld *et al.*
 839 2009; Speijer 2016; **Figure 2**). The dependence of ROX-linked O₂ consumption needs to be
 840 studied in detail together with non-ET enzyme activities, availability of specific substrates, O₂
 841 concentration, and electron leakage leading to the formation of reactive oxygen species.

842 **Quantitative relations:** *E* may exceed or be equal to *P*. *E* > *P* is observed in many types
 843 of mitochondria, varying between species, tissues and cell types (Gnaiger 2009). *E-P* is the
 844 excess ET-capacity pushing the phosphorylation-flux (**Figure 2C**) to the limit of its *capacity of*
 845 *utilizing* the protonmotive force. In addition, the magnitude of *E-P* depends on the tightness of
 846 respiratory coupling or degree of uncoupling, since an increase of *L* causes *P* to increase
 847 towards the limit of *E*. The *excess E-P* capacity, *E-P*, therefore, provides a sensitive diagnostic
 848 indicator of specific injuries of the phosphorylation-pathway, under conditions when *E* remains
 849 constant but *P* declines relative to controls (**Figure 5**). Substrate cocktails supporting
 850 simultaneous convergent electron transfer to the Q-junction for reconstitution of TCA cycle
 851 function establish pathway control states with high ET-capacity, and consequently increase the
 852 sensitivity of the *E-P* assay.

853 *E* cannot theoretically be lower than *P*. *E* < *P* must be discounted as an artefact, which
 854 may be caused experimentally by: (1) loss of oxidative capacity during the time course of the
 855 respirometric assay, since *E* is measured subsequently to *P*; (2) using insufficient uncoupler
 856 concentrations; (3) using high uncoupler concentrations which inhibit ET (Gnaiger 2008); (4)
 857 high oligomycin concentrations applied for measurement of *L* before titrations of uncoupler,
 858 when oligomycin exerts an inhibitory effect on *E*. On the other hand, the excess ET-capacity is
 859 overestimated if non-saturating [ADP] or [P_i] are used. See State 3 in the next section.

860 The net OXPHOS-capacity is calculated by subtracting *L* from *P* (**Figure 5**). The net
 861 $P \gg O_2$ equals $P \gg (P-L)$, wherein the dissipative LEAK component in the OXPHOS-state may
 862 be overestimated. This can be avoided by measuring LEAK-respiration in a state when the
 863 protonmotive force is adjusted to its slightly lower value in the OXPHOS-state—by titration of
 864 an ET inhibitor (Divakaruni and Brand 2011). Any turnover-dependent components of proton
 865 leak and slip, however, are underestimated under these conditions (Garlid *et al.* 1993). In
 866 general, it is inappropriate to use the term *ATP production* or *ATP turnover* for the difference
 867 of O₂ flux measured in the OXPHOS and LEAK states. *P-L* is the upper limit of OXPHOS-
 868 capacity that is freely available for ATP production (corrected for LEAK-respiration) and is
 869 fully coupled to phosphorylation with a maximum mechanistic stoichiometry (**Figure 5**).

870 The rates of LEAK respiration and OXPHOS capacity depend on (1) the tightness of
 871 coupling under the influence of the respiratory uncoupling mechanisms (**Figure 4**), and (2) the
 872 coupling stoichiometry, which varies as a function of the substrate type undergoing oxidation
 873 in ET-pathways with either two or three coupling sites (**Figure 2B**). When cocktails with
 874 NADH-linked substrates and succinate are used, the relative contribution of ET-pathways with
 875 three or two coupling sites cannot be controlled experimentally, is difficult to determine, and
 876 may shift in transitions between LEAK-, OXPHOS- and ET-states (Gnaiger 2014). Under these
 877 experimental conditions, we cannot separate the tightness of coupling *versus* coupling
 878 stoichiometry as the mechanisms of respiratory control in the shift of *L/P* ratios. The tightness

879 of coupling and fully coupled O₂ flux, *P-L* (**Table 2**), therefore, are obtained from
 880 measurements of coupling control of LEAK respiration, OXPHOS- and ET-capacities in well
 881 defined pathway states, using either pyruvate and malate as substrates or the classical succinate
 882 and rotenone substrate-inhibitor combination (**Figure 2B**).

883

884 2.3. Classical terminology for isolated mitochondria

885 *'When a code is familiar enough, it ceases appearing like a code; one forgets that there*
 886 *is a decoding mechanism. The message is identical with its meaning'* (Hofstadter 1979).

887

888 Chance and Williams (1955; 1956) introduced five classical states of mitochondrial
 889 respiration and cytochrome redox states. **Table 3** shows a protocol with isolated mitochondria
 890 in a closed respirometric chamber, defining a sequence of respiratory states. States and rates
 891 are not specifically distinguished in this nomenclature.

892

893

Table 3. Metabolic states of mitochondria (Chance and Williams, 1956; Table V).

State	[O ₂]	ADP level	Substrate Level	Respiration rate	Rate-limiting substance
1	>0	low	Low	slow	ADP
2	>0	high	~0	slow	substrate
3	>0	high	high	fast	respiratory chain
4	>0	low	high	slow	ADP
5	0	high	high	0	oxygen

896

897 **State 1** is obtained after addition of isolated mitochondria to air-saturated
 898 isoosmotic/isotonic respiration medium containing P_i, but no fuel substrates and no adenylates,
 899 *i.e.*, AMP, ADP, ATP.

900 **State 2** is induced by addition of a 'high' concentration of ADP (typically 100 to 300
 901 μM), which stimulates respiration transiently on the basis of endogenous fuel substrates and
 902 phosphorylates only a small portion of the added ADP. State 2 is then obtained at a low
 903 respiratory activity limited by exhausted endogenous fuel substrate availability (**Table 3**). If
 904 addition of specific inhibitors of respiratory complexes—such as rotenone—does not cause a
 905 further decline of O₂ flux, State 2 is equivalent to the ROX state (See below.). If inhibition is
 906 observed, undefined endogenous fuel substrates are a confounding factor of pathway control,
 907 contributing to the effect of subsequently externally added substrates and inhibitors. In contrast
 908 to the original protocol, an alternative sequence of titration steps is frequently applied, in which
 909 the alternative 'State 2' has an entirely different meaning, when this second state is induced by
 910 addition of fuel substrate without ADP (LEAK-state; in contrast to State 2 defined in **Table 1**
 911 as a ROX state), followed by addition of ADP.

912 **State 3** is the state stimulated by addition of fuel substrates while the ADP concentration
 913 is still high (**Table 3**) and supports coupled energy transformation through oxidative
 914 phosphorylation. 'High ADP' is a concentration of ADP specifically selected to allow the
 915 measurement of State 3 to State 4 transitions of isolated mitochondria in a closed respirometric
 916 chamber. Repeated ADP titration re-establishes State 3 at 'high ADP'. Starting at O₂
 917 concentrations near air-saturation (ca. 200 μM O₂ at sea level and 37 °C), the total ADP
 918 concentration added must be low enough (typically 100 to 300 μM) to allow phosphorylation
 919 to ATP at a coupled O₂ flux that does not lead to O₂ depletion during the transition to State 4.
 920 In contrast, kinetically-saturating ADP concentrations usually are 10-fold higher than 'high
 921 ADP', *e.g.*, 2.5 mM in isolated mitochondria. The abbreviation State 3u is occasionally used in
 922 bioenergetics, to indicate the state of respiration after titration of an uncoupler, without

923 sufficient emphasis on the fundamental difference between OXPHOS-capacity (*well-coupled*
924 with an *endogenous* uncoupled component) and ET-capacity (*noncoupled*).

925 **State 4** is a LEAK-state that is obtained only if the mitochondrial preparation is intact
926 and well-coupled. Depletion of ADP by phosphorylation to ATP causes a decline of O₂ flux in
927 the transition from State 3 to State 4. Under the conditions of State 4, a maximum protonmotive
928 force and high ATP/ADP ratio are maintained. The gradual decline of $Y_{P\gg/O_2}$ towards
929 diminishing [ADP] at State 4 must be taken into account for calculation of P \gg /O₂ ratios (Gnaiger
930 2001). State 4 respiration, L_T (**Table 1**), reflects intrinsic proton leak and ATP hydrolysis
931 activity. O₂ flux in State 4 is an overestimation of LEAK-respiration if the contaminating ATP
932 hydrolysis activity recycles some ATP to ADP, $J_{P\ll}$, which stimulates respiration coupled to
933 phosphorylation, $J_{P\gg} > 0$. This can be tested by inhibition of the phosphorylation-pathway using
934 oligomycin, ensuring that $J_{P\gg} = 0$ (State 4o). Alternatively, sequential ADP titrations re-
935 establish State 3, followed by State 3 to State 4 transitions while sufficient O₂ is available.
936 Anoxia may be reached, however, before exhaustion of ADP (State 5).

937 **State 5** is the state after exhaustion of O₂ in a closed respirometric chamber. Diffusion of
938 O₂ from the surroundings into the aqueous solution may be a confounding factor preventing
939 complete anoxia (Gnaiger 2001). Chance and Williams (1955) provide an alternative definition
940 of State 5, which gives it the different meaning of ROX versus anoxia: ‘State 5 may be obtained
941 by antimycin A treatment or by anaerobiosis’.

942 In **Table 3**, only States 3 and 4 (and ‘State 2’ in the alternative protocol: addition of fuel
943 substrates without ADP; not included in the table) are coupling control states, with the
944 restriction that O₂ flux in State 3 may be limited kinetically by non-saturating ADP
945 concentrations (**Table 1**).

946
947

948 3. Normalization: flows and fluxes

949

950 3.1. Normalization: system or sample

951

952 The term *rate* is not sufficiently defined to be useful for reporting data (**Figure 7**). The
953 inconsistency of the meanings of rate becomes fully apparent when considering Galileo
954 Galilei’s famous principle, that ‘bodies of different weight all fall at the same rate (have a
955 constant acceleration)’ (Coopersmith 2010).

956 **Flow per system, I** : In a generalization of electrical terms, flow as an extensive quantity
957 (I ; per system) is distinguished from flux as a size-specific quantity (J ; per system size) (**Figure**
958 **7A**). Electric current is flow, I_{el} [$A \equiv C \cdot s^{-1}$] per system (extensive quantity). When dividing this
959 extensive quantity by system size (cross-sectional area of a ‘wire’), a size-specific quantity is
960 obtained, which is flux (current density), J_{el} [$A \cdot m^{-2} = C \cdot s^{-1} \cdot m^{-2}$] (**Box 2**).

961

962
963

964 **Box 2: Metabolic flows and fluxes: vectorial and scalar**

965

964 *Flows, I_{tr}* , are defined for all transformations as extensive quantities. Electric charge per
965 unit time is electric flow or current, $I_{el} = dQ_{el} \cdot dt^{-1}$ [A]. When expressed per unit cross-sectional
966 area, A [m^2], a vector flux is obtained, which is current density (surface-density of flow)
967 perpendicular to the direction of flux, $J_{el} = I_{el} \cdot A^{-1}$ [$A \cdot m^{-2}$] (Cohen et al. 2008). Fluxes with
968 *spatial* geometric direction and magnitude are *vectors*. Vector and scalar *fluxes* are related to
969 flows as $J_{tr} = I_{tr} \cdot A^{-1}$ [$mol \cdot s^{-1} \cdot m^{-2}$] and $J_{tr} = I_{tr} \cdot V^{-1}$ [$mol \cdot s^{-1} \cdot m^{-3}$], expressing flux as an area-specific
970 vector or volume-specific vectorial or scalar quantity, respectively (Gnaiger 1993b). We use
971 the metre–kilogram–second–ampere (MKSA) international system of units (*SI*) for general
972 cases ([m], [kg], [s] and [A]), with decimal *SI* prefixes for specific applications (**Table 4**).

973

974 We suggest to define: (1) *vectorial* fluxes, which are translocations as functions of
gradients with direction in geometric space in continuous systems; (2) *vectorial* fluxes, which

975 describe translocations in discontinuous systems and are restricted to information on
 976 *compartmental differences* (**Figure 3**, transmembrane proton flux); and (3) *scalar* fluxes, which
 977 are transformations in a *homogenous* system (**Figure 3**, catabolic O₂ flux, J_{kO_2}).

978 Vectorial transmembrane proton fluxes, J_{mH^+pos} and J_{mH^+neg} , are analyzed in a
 979 heterogenous compartmental system as a quantity with *directional* but not *spatial* information.
 980 Translocation of protons across the mtIM has a defined direction, either from the negative
 981 compartment (matrix space; negative, neg-compartment) to the positive compartment (inter-
 982 membrane space; positive, pos-compartment) or *vice versa* (**Figure 3**). The arrows defining
 983 the direction of the translocation between the two vesicular compartments may point upwards
 984 or downwards, right or left, without any implication that these are actual directions in space.
 985 The pos-compartment is neither above nor below the neg-compartment in a spatial sense, but
 986 can be visualized arbitrarily in a figure in the upper position (**Figure 3**). In general, the
 987 *compartmental direction* of vectorial translocation from the neg-compartment to the pos-
 988 compartment is defined by assigning the initial and final state as *ergodynamic compartments*,
 989 $H^+_{neg} \rightarrow H^+_{pos}$ or $0 = -1 H^+_{neg} + 1 H^+_{pos}$, related to work (erg = work) that must be performed to
 990 lift the proton from a lower to a higher electrochemical potential or from the lower to the higher
 991 ergodynamic compartment (Gnaiger 1993b).

992 In analogy to *vectorial* translocation, the direction of a *scalar* chemical reaction, $A \rightarrow B$
 993 or $0 = -1 A + 1 B$, is defined by assigning substrates and products, A and B, as ergodynamic
 994 compartments. O₂ is defined as a substrate in respiratory O₂ consumption (electron acceptor),
 995 which together with the fuel substrates (electron donors) comprises the substrate compartment
 996 of the catabolic reaction. Volume-specific scalar O₂ flux is coupled to vectorial translocation,
 997 yielding the H^+_{pos}/O_2 ratio (**Figure 2B**).

998
 999 **Extensive quantities:** An extensive quantity increases proportionally with system size.
 1000 The magnitude of an extensive quantity is completely additive for non-interacting
 1001 subsystems—such as mass or flow expressed per defined system. The magnitude of these
 1002 quantities depends on the extent or size of the system (Cohen *et al.* 2008).

1003 **Size-specific quantities:** ‘The adjective *specific* before the name of an extensive quantity
 1004 is often used to mean *divided by mass*’ (Cohen *et al.* 2008). In this system-paradigm, mass-
 1005 specific flux is flow divided by mass of the *system* (the total mass of everything within the
 1006 measuring chamber or reactor). A mass-specific quantity is independent of the extent of non-
 1007 interacting homogenous subsystems. Tissue-specific quantities (related to the *sample* in
 1008 contrast to the *system*) are of fundamental interest in the field of comparative mitochondrial
 1009 physiology, where *specific* refers to the *type of the sample* rather than *mass of the system*. The
 1010 term *specific*, therefore, must be clarified; *sample-specific*, e.g., muscle mass-specific
 1011 normalization, is distinguished from *system-specific* quantities (mass or volume; **Figure 7**).

1012
 1013 *3.2. Normalization for system-size: flux per chamber volume*

1014
 1015 **System-specific flux, J_{V,O_2} :** The experimental system (experimental chamber) is part of
 1016 the measurement apparatus, separated from the environment as an isolated, closed, open,
 1017 isothermal or non-isothermal system (**Table 4**). On another level, we distinguish between (1)
 1018 the *system* with volume V and mass m defined by the system boundaries, and (2) the *sample* or
 1019 *objects* with volume V_X and mass m_X that are enclosed in the experimental chamber (**Figure 7**).
 1020 Metabolic O₂ flow per object, $I_{O_2/X}$, increases as the mass of the object is increased. Sample
 1021 mass-specific O₂ flux, $J_{O_2/mX}$ should be independent of the mass of the sample studied in the
 1022 instrument chamber, but system volume-specific O₂ flux, J_{V,O_2} (per volume of the instrument
 1023 chamber), should increase in direct proportion to the mass of the sample in the chamber.
 1024 Whereas J_{V,O_2} depends on mass-concentration of the sample in the chamber, it should be
 1025 independent of the chamber (system) volume at constant sample mass. There are practical

1026 limitations to increase the mass-concentration of the sample in the chamber, when one is
 1027 concerned about crowding effects and instrumental time resolution.

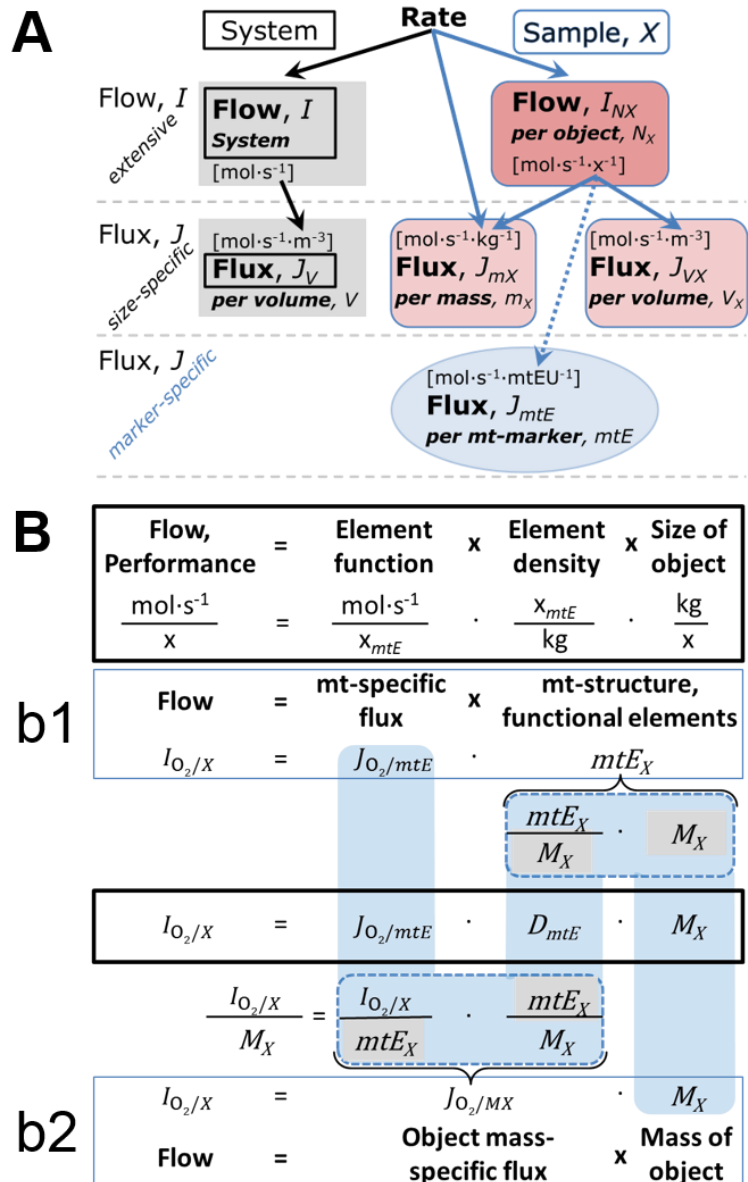
1028
 1029 **Figure 7. Flow and flux, and**
 1030 **normalization in structure-**
 1031 **function analysis**

1032 (A) Different meanings of rate
 1033 may lead to confusion, if the
 1034 normalization is not sufficiently
 1035 specified. Results are frequently
 1036 expressed as mass-specific *flux*,
 1037 J_{mX} , per mg protein, dry or wet
 1038 weight (mass). Cell volume, V_{cell} ,
 1039 may be used for normalization
 1040 (volume-specific flux, $J_{V\text{cell}}$),
 1041 which must be clearly
 1042 distinguished from flow per cell,
 1043 $I_{N\text{cell}}$, or flux, J_V , expressed for
 1044 methodological reasons per
 1045 volume of the measurement
 1046 system.

1047 (B) O_2 flow, $I_{\text{O}_2/X}$, is the product
 1048 of performance per functional
 1049 element (element function,
 1050 mitochondria-specific flux),
 1051 element density (mitochondrial
 1052 density, D_{mtE}), and size of entity X
 1053 (mass, M_X). (b1) Structured
 1054 analysis: performance is the
 1055 product of mitochondrial *function*
 1056 (mt-specific flux) and *structure*
 1057 (functional elements; D_{mtE} times
 1058 mass of X). (b2) Unstructured
 1059 analysis: performance is the
 1060 product of *entity mass-specific*
 1061 flux, $J_{\text{O}_2/MX} = I_{\text{O}_2/X}/M_X = I_{\text{O}_2}/m_X$
 1062 $[\text{mol}\cdot\text{s}^{-1}\cdot\text{kg}^{-1}]$ and *size of entity*,
 1063 expressed as mass of X ; $M_X = m_X \cdot N_X^{-1}$ $[\text{kg}\cdot\text{x}^{-1}]$. Modified from
 1064 Gnaiger (2014). For further details see **Table 4**.

1065
 1066
 1067
 1068
 1069
 1070
 1071
 1072
 1073
 1074
 1075
 1076

When the reactor volume does not change during the reaction, which is typical for liquid phase reactions, the volume-specific flux of a chemical reaction r is the time derivative of the advancement of the reaction per unit volume, $J_{V,rB} = d_{r\zeta_B}/dt \cdot V^{-1}$ $[(\text{mol}\cdot\text{s}^{-1})\cdot\text{L}^{-1}]$. The rate of concentration change is dc_B/dt $[(\text{mol}\cdot\text{L}^{-1})\cdot\text{s}^{-1}]$, where concentration is $c_B = n_B/V$. There is a difference between (1) $J_{V,r\text{O}_2}$ $[\text{mol}\cdot\text{s}^{-1}\cdot\text{L}^{-1}]$ and (2) rate of concentration change $[\text{mol}\cdot\text{L}^{-1}\cdot\text{s}^{-1}]$. These merge to a single expression only in closed systems. In open systems, external fluxes (such as O_2 supply) are distinguished from internal transformations (catabolic flux, O_2 consumption). In a closed system, external flows of all substances are zero and O_2 consumption (internal flow of catabolic reactions k), $I_{k\text{O}_2}$ $[\text{pmol}\cdot\text{s}^{-1}]$, causes a decline of the amount of O_2 in the system, n_{O_2} $[\text{nmol}]$. Normalization of these quantities for the volume of the system, V $[\text{L} \equiv \text{dm}^3]$, yields volume-specific O_2 flux, $J_{V,k\text{O}_2} = I_{k\text{O}_2}/V$ $[\text{nmol}\cdot\text{s}^{-1}\cdot\text{L}^{-1}]$, and O_2 concentration, $[\text{O}_2]$ or $c_{\text{O}_2} = n_{\text{O}_2}/V$ $[\mu\text{mol}\cdot\text{L}^{-1} = \mu\text{M} = \text{nmol}\cdot\text{mL}^{-1}]$. Instrumental background O_2 flux is due to external



1077 flux into a non-ideal closed respirometer; then total volume-specific flux has to be corrected for
 1078 instrumental background O₂ flux—O₂ diffusion into or out of the instrumental chamber. J_{V,kO_2}
 1079 is relevant mainly for methodological reasons and should be compared with the accuracy of
 1080 instrumental resolution of background-corrected flux, *e.g.*, $\pm 1 \text{ nmol}\cdot\text{s}^{-1}\cdot\text{L}^{-1}$ (Gnaiger 2001).
 1081 ‘Metabolic’ or catabolic indicates O₂ flux, J_{kO_2} , corrected for: (1) instrumental background O₂
 1082 flux; (2) chemical background O₂ flux due to autoxidation of chemical components added to
 1083 the incubation medium; and (3) R_{ox} for O₂-consuming side reactions unrelated to the catabolic
 1084 pathway *k*.

1085

1086 3.3. Normalization: per sample

1087

1088 The challenges of measuring mitochondrial respiratory flux are matched by those of
 1089 normalization. Application of common and defined units is required for direct transfer of
 1090 reported results into a database. The second [s] is the *SI* unit for the base quantity *time*. It is also
 1091 the standard time-unit used in solution chemical kinetics. A rate may be considered as the
 1092 numerator and normalization as the complementary denominator, which are tightly linked in
 1093 reporting the measurements in a format commensurate with the requirements of a database.
 1094 Normalization (**Table 4**) is guided by physicochemical principles, methodological
 1095 considerations, and conceptual strategies (**Figure 7**).

1096 **Sample concentration, C_{mX} :** Normalization for sample concentration is required to
 1097 report respiratory data. Considering a tissue or cells as the sample, *X*, the sample mass is m_X
 1098 [mg], which is frequently measured as wet or dry weight, W_w or W_d [mg], respectively, or as
 1099 amount of tissue or cell protein, m_{Protein} . In the case of permeabilized tissues, cells, and
 1100 homogenates, the sample concentration, $C_{mX} = m_X/V$ [$\text{g}\cdot\text{L}^{-1} = \text{mg}\cdot\text{mL}^{-1}$], is the mass of the
 1101 subsample of tissue that is transferred into the instrument chamber.

1102 **Mass-specific flux, $J_{O_2/mX}$:** Mass-specific flux is obtained by expressing respiration per
 1103 mass of sample, m_X [mg]. *X* is the type of sample—isolated mitochondria, tissue homogenate,
 1104 permeabilized fibres or cells. Volume-specific flux is divided by mass concentration of *X*, $J_{O_2/mX}$
 1105 $= J_{V,O_2}/C_{mX}$; or flow per cell is divided by mass per cell, $J_{O_2/m_{\text{cell}}} = I_{O_2/\text{cell}}/M_{\text{cell}}$. If mass-specific
 1106 O₂ flux is constant and independent of sample size (expressed as mass), then there is no
 1107 interaction between the subsystems. A 1.5 mg and a 3.0 mg muscle sample respire at identical
 1108 mass-specific flux. Mass-specific O₂ flux, however, may change with the mass of a tissue
 1109 sample, cells or isolated mitochondria in the measuring chamber, in which the nature of the
 1110 interaction becomes an issue. Therefore, cell density must be optimized, particularly in
 1111 experiments carried out in wells, considering the confluency of the cell monolayer or clumps
 1112 of cells (Salabei *et al.* 2014).

1113 **Number concentration, C_{NX} :** C_{NX} is the experimental *number concentration* of sample
 1114 *X*. In the case of cells or animals, *e.g.*, nematodes, $C_{NX} = N_X/V$ [$\text{x}\cdot\text{L}^{-1}$], where N_X is the number
 1115 of cells or organisms in the chamber (**Table 4**).

1116 **Flow per object, $I_{O_2/X}$:** A special case of normalization is encountered in respiratory
 1117 studies with permeabilized (or intact) cells. If respiration is expressed per cell, the O₂ flow per
 1118 measurement system is replaced by the O₂ flow per cell, $I_{O_2/\text{cell}}$ (**Table 4**). O₂ flow can be
 1119 calculated from volume-specific O₂ flux, J_{V,O_2} [$\text{nmol}\cdot\text{s}^{-1}\cdot\text{L}^{-1}$] (per *V* of the measurement chamber
 1120 [L]), divided by the number concentration of cells, $C_{N_{\text{cell}}} = N_{\text{cell}}/V$ [$\text{cell}\cdot\text{L}^{-1}$], where N_{cell} is the
 1121 number of cells in the chamber. The total cell count is the sum of viable and dead cells, $N_{\text{cell}} =$
 1122 $N_{\text{vce}} + N_{\text{dce}}$ (**Table 5**). The cell viability index, $\text{CVI} = N_{\text{vce}}/N_{\text{cell}}$, is the ratio of viable cells (N_{vce} ;
 1123 before experimental permeabilization) per total cell count. After experimental permeabilization,
 1124 all cells are permeabilized, $N_{\text{pce}} = N_{\text{cell}}$. The cell viability index can be used to normalize
 1125 respiration for the number of cells that have been viable before experimental permeabilization,
 1126 $I_{O_2/\text{vce}} = I_{O_2/\text{cell}}/\text{CVI}$, considering that mitochondrial respiratory dysfunction in dead cells should
 1127 be eliminated as a confounding factor.

Table 4. Sample concentrations and normalization of flux.

Expression	Symbol	Definition	Unit	Notes
Sample				
identity of sample	X	object: cell, tissue, animal, patient		
number of sample entities X	N_X	number of objects	x	
mass of sample X	m_X		kg	1
mass of object X	M_X	$M_X = m_X \cdot N_X^{-1}$	$\text{kg} \cdot \text{x}^{-1}$	1
Mitochondria				
mitochondria	mt	$X = \text{mt}$		
amount of mt-elements	mtE	quantity of mt-marker	mtEU	
Concentrations				
object number concentration	C_{NX}	$C_{NX} = N_X \cdot V^{-1}$	$\text{x} \cdot \text{m}^{-3}$	2
sample mass concentration	C_{mX}	$C_{mX} = m_X \cdot V^{-1}$	$\text{kg} \cdot \text{m}^{-3}$	
mitochondrial concentration	C_{mtE}	$C_{mtE} = mtE \cdot V^{-1}$	$\text{mtEU} \cdot \text{m}^{-3}$	3
specific mitochondrial density	D_{mtE}	$D_{mtE} = mtE \cdot m_X^{-1}$	$\text{mtEU} \cdot \text{kg}^{-1}$	4
mitochondrial content, mtE per object X	mtE_X	$mtE_X = mtE \cdot N_X^{-1}$	$\text{mtEU} \cdot \text{x}^{-1}$	5
O₂ flow and flux				
flow, system	I_{O_2}	internal flow	$\text{mol} \cdot \text{s}^{-1}$	6
volume-specific flux	J_{V,O_2}	$J_{V,O_2} = I_{O_2} \cdot V^{-1}$	$\text{mol} \cdot \text{s}^{-1} \cdot \text{m}^{-3}$	7
flow per object X	$I_{O_2/X}$	$I_{O_2/X} = J_{V,O_2} \cdot C_{NX}^{-1}$	$\text{mol} \cdot \text{s}^{-1} \cdot \text{x}^{-1}$	8
mass-specific flux	$J_{O_2/mX}$	$J_{O_2/mX} = J_{V,O_2} \cdot C_{mX}^{-1}$	$\text{mol} \cdot \text{s}^{-1} \cdot \text{kg}^{-1}$	9
mitochondria-specific flux	$J_{O_2/mtE}$	$J_{O_2/mtE} = J_{V,O_2} \cdot C_{mtE}^{-1}$	$\text{mol} \cdot \text{s}^{-1} \cdot \text{mtEU}^{-1}$	10

- 1130 1 Units are given in the MKSA system (**Box 2**). The *SI* prefix k is used for the *SI* base unit of mass (kg
1131 = 1,000 g). In praxis, various *SI* prefixes are used for convenience, to make numbers easily readable,
1132 e.g., 1 mg tissue, cell or mitochondrial mass instead of 0.000001 kg.
- 1133 2 In case sample $X = \text{cells}$, the object number concentration is $C_{N_{\text{cell}}} = N_{\text{cell}} \cdot V^{-1}$, and volume may be
1134 expressed in [$\text{dm}^3 \equiv \text{L}$] or [$\text{cm}^3 = \text{mL}$]. See **Table 5** for different object types.
- 1135 3 mt-concentration is an experimental variable, dependent on sample concentration: (1) $C_{mtE} = mtE \cdot V^{-1}$;
1136 (2) $C_{mtE} = mtE_X \cdot C_{NX}$; (3) $C_{mtE} = C_{mX} \cdot D_{mtE}$.
- 1137 4 If the amount of mitochondria, mtE , is expressed as mitochondrial mass, then D_{mtE} is the mass
1138 fraction of mitochondria in the sample. If mtE is expressed as mitochondrial volume, V_{mt} , and the
1139 mass of sample, m_X , is replaced by volume of sample, V_X , then D_{mtE} is the volume fraction of
1140 mitochondria in the sample.
- 1141 5 $mtE_X = mtE \cdot N_X^{-1} = C_{mtE} \cdot C_{NX}^{-1}$.
- 1142 6 O₂ can be replaced by other chemicals B to study different reactions, e.g., ATP, H₂O₂, or vesicular
1143 compartmental translocations, e.g., Ca²⁺.
- 1144 7 I_{O_2} and V are defined per instrument chamber as a system of constant volume (and constant
1145 temperature), which may be closed or open. I_{O_2} is abbreviated for I_{r,O_2} , i.e., the metabolic or internal
1146 O₂ flow of the chemical reaction r in which O₂ is consumed, hence the negative stoichiometric
1147 number, $\nu_{O_2} = -1$. $I_{r,O_2} = d_r n_{O_2} / dt \cdot \nu_{O_2}^{-1}$. If r includes all chemical reactions in which O₂ participates, then
1148 $d_r n_{O_2} = dn_{O_2} - d_e n_{O_2}$, where dn_{O_2} is the change in the amount of O₂ in the instrument chamber and $d_e n_{O_2}$
1149 is the amount of O₂ added externally to the system. At steady state, by definition $dn_{O_2} = 0$, hence $d_r n_{O_2}$
1150 $= -d_e n_{O_2}$.
- 1151 8 J_{V,O_2} is an experimental variable, expressed per volume of the instrument chamber.
- 1152 9 $I_{O_2/X}$ is a physiological variable, depending on the size of entity X .
- 1153 10 There are many ways to normalize for a mitochondrial marker, that are used in different experimental
1154 approaches: (1) $J_{O_2/mtE} = J_{V,O_2} \cdot C_{mtE}^{-1}$; (2) $J_{O_2/mtE} = J_{V,O_2} \cdot C_{mX}^{-1} \cdot D_{mtE}^{-1} = J_{O_2/mX} \cdot D_{mtE}^{-1}$; (3) $J_{O_2/mtE} =$
1155 $J_{V,O_2} \cdot C_{NX}^{-1} \cdot mtE_X^{-1} = I_{O_2/X} \cdot mtE_X^{-1}$; (4) $J_{O_2/mtE} = I_{O_2} \cdot mtE^{-1}$. The mt-elemental unit [mtEU] varies between
1156 different mt-markers.

1157
1158**Table 5. Sample types, X, abbreviations, and quantification.**

Identity of sample	X	N_X	Mass ^a	Volume	mt-Marker
mitochondrial preparation	mt-prep	[x]	[kg]	[m ³]	[mtEU]
isolated mitochondria	imt		m_{mt}	V_{mt}	mtE
tissue homogenate	thom		m_{thom}		mtE_{thom}
permeabilized tissue	pti		m_{pti}		mtE_{pti}
permeabilized fibre	pfi		m_{pfi}		mtE_{pfi}
permeabilized cell	pce	N_{pce}	M_{pce}	V_{pce}	mtE_{pce}
cells ^b	cell	N_{cell}	M_{cell}	V_{cell}	mtE_{cell}
intact cell, viable cell	vce	N_{vce}	M_{vce}	V_{vce}	
dead cell	dce	N_{dce}	M_{dce}	V_{dce}	
organism	org	N_{org}	M_{org}	V_{org}	

1159 ^a Instead of mass, the wet weight or dry weight is frequently stated, W_w or W_d .1160 m_X is mass of the sample [kg], M_X is mass of the object [$kg \cdot x^{-1}$].1161 ^b Total cell count, $N_{cell} = N_{vce} + N_{dce}$ 1162
11631164 Cellular O₂ flow can be compared between cells of identical size. To take into account
1165 changes and differences in cell size, normalization is required to obtain cell size-specific or
1166 mitochondrial marker-specific O₂ flux (Renner *et al.* 2003).1167 The complexity changes when the sample is a whole organism studied as an experimental
1168 model. The scaling law in respiratory physiology reveals a strong interaction of O₂ flow and
1169 individual body mass of an organism, since *basal* metabolic rate (flow) does not increase
1170 linearly with body mass, whereas *maximum* mass-specific O₂ flux, \dot{V}_{O_2max} or \dot{V}_{O_2peak} , is
1171 approximately constant across a large range of individual body mass (Weibel and Hoppeler
1172 2005), with individuals, breeds, and species deviating substantially from this relationship. For
1173 comparison of units, \dot{V}_{O_2peak} of human endurance athletes is 60 to 80 mL O₂·min⁻¹·kg⁻¹ body
1174 mass, converted to $J_{O_2peak/M}$ of 45 to 60 nmol·s⁻¹·g⁻¹ (Gnaiger 2014; **Table 6**).

1175

1176

3.4. Normalization for mitochondrial content

1177

1178 Tissues can contain multiple cell populations that may have distinct mitochondrial
1179 subtypes. Mitochondria undergo dynamic fission and fusion cycles, and can exist in multiple
1180 stages and sizes that may be altered by a range of factors. The isolation of mitochondria (often
1181 achieved through differential centrifugation) can therefore yield a subsample of the
1182 mitochondrial types present in a tissue, depending on the isolation protocols utilized (*e.g.*,
1183 centrifugation speed). This possible bias should be taken into account when planning
1184 experiments using isolated mitochondria. Different sizes of mitochondria are enriched at
1185 specific centrifugation speeds, which can be used strategically for isolation of mitochondrial
1186 subpopulations.1187 Part of the mitochondrial content of a tissue is lost during preparation of isolated
1188 mitochondria. The fraction of isolated mitochondria obtained from a tissue sample is expressed
1189 as mitochondrial recovery. At a high mitochondrial recovery the fraction of isolated
1190 mitochondria is more representative of the total mitochondrial population than in preparations
1191 characterized by low recovery. Determination of the mitochondrial recovery and yield is based
1192 on measurement of the concentration of a mitochondrial marker in the stock of isolated
1193 mitochondria, $C_{mtE,stock}$, and crude tissue homogenate, $C_{mtE,thom}$, which simultaneously provides
1194 information on the specific mitochondrial density in the sample, D_{mtE} (**Table 4**).

1195 Normalization is a problematic subject; it is essential to consider the question of the study.
 1196 If the study aims at comparing tissue performance—such as the effects of a treatment on a
 1197 specific tissue, then normalization for tissue mass or protein content is appropriate. However,
 1198 if the aim is to find differences on mitochondrial function independent of mitochondrial density
 1199 (**Table 4**), then normalization to a mitochondrial marker is imperative (**Figure 7**). One cannot
 1200 assume that quantitative changes in various markers—such as mitochondrial proteins—
 1201 necessarily occur in parallel with one another. It should be established that the marker chosen
 1202 is not selectively altered by the performed treatment. In conclusion, the normalization must
 1203 reflect the question under investigation to reach a satisfying answer. On the other hand, the goal
 1204 of comparing results across projects and institutions requires standardization on normalization
 1205 for entry into a databank.

1206 **Mitochondrial concentration, C_{mtE} , and mitochondrial markers:** Mitochondrial
 1207 organelles comprise a dynamic cellular reticulum in various states of fusion and fission. Hence,
 1208 the definition of an "amount" of mitochondria is often misconceived: mitochondria cannot be
 1209 counted reliably as a number of occurring elements. Therefore, quantification of the "amount"
 1210 of mitochondria depends on the measurement of chosen mitochondrial markers. 'Mitochondria
 1211 are the structural and functional elemental units of cell respiration' (Gnaiger 2014). The
 1212 quantity of a mitochondrial marker can reflect the amount of *mitochondrial elements, mtE*,
 1213 expressed in various mitochondrial elemental units [mtEU] specific for each measured mt-
 1214 marker (**Table 4**). However, since mitochondrial quality may change in response to stimuli—
 1215 particularly in mitochondrial dysfunction (Campos *et al.* 2017) and after exercise training (Pesta
 1216 *et al.* 2011) and during aging (Daum *et al.* 2013)—some markers can vary while others are
 1217 unchanged: (1) Mitochondrial volume and membrane area are structural markers, whereas
 1218 mitochondrial protein mass is frequently used as a marker for isolated mitochondria. (2)
 1219 Molecular and enzymatic mitochondrial markers (amounts or activities) can be selected as
 1220 matrix markers, *e.g.*, citrate synthase activity, mtDNA; mtIM-markers, *e.g.*, cytochrome *c*
 1221 oxidase activity, *aa₃* content, cardiolipin, or mtOM-markers, *e.g.*, the voltage-dependent anion
 1222 channel (VDAC), TOM20. (3) Extending the measurement of mitochondrial marker enzyme
 1223 activity to mitochondrial pathway capacity, ET- or OXPHOS-capacity can be considered as an
 1224 integrative functional mitochondrial marker.

1225 Depending on the type of mitochondrial marker, the mitochondrial elements, *mtE*, are
 1226 expressed in marker-specific units. Mitochondrial concentration in the measurement chamber
 1227 and the tissue of origin are quantified as (1) a quantity for normalization in functional analyses,
 1228 C_{mtE} , and (2) a physiological output that is the result of mitochondrial biogenesis and
 1229 degradation, D_{mtE} , respectively (**Table 4**). It is recommended, therefore, to distinguish
 1230 *experimental mitochondrial concentration*, $C_{mtE} = mtE/V$ and *physiological mitochondrial*
 1231 *density*, $D_{mtE} = mtE/m_X$. Then mitochondrial density is the amount of mitochondrial elements
 1232 per mass of tissue, which is a biological variable (**Figure 7**). The experimental variable is
 1233 mitochondrial density multiplied by sample mass concentration in the measuring chamber, C_{mtE}
 1234 $= D_{mtE} \cdot C_{mX}$, or mitochondrial content multiplied by sample number concentration, $C_{mtE} =$
 1235 $mtE_X \cdot C_{NX}$ (**Table 4**).

1236 **Mitochondria-specific flux, $J_{O_2/mtE}$:** Volume-specific metabolic O_2 flux depends on: (1)
 1237 the sample concentration in the volume of the instrument chamber, C_{mX} , or C_{NX} ; (2) the
 1238 mitochondrial density in the sample, $D_{mtE} = mtE/m_X$ or $mtE_X = mtE/N_X$; and (3) the specific
 1239 mitochondrial activity or performance per elemental mitochondrial unit, $J_{O_2/mtE} = J_{V,O_2}/C_{mtE}$
 1240 [$\text{mol} \cdot \text{s}^{-1} \cdot \text{mtEU}^{-1}$] (**Table 4**). Obviously, the numerical results for $J_{O_2/mtE}$ vary with the type of
 1241 mitochondrial marker chosen for measurement of *mtE* and $C_{mtE} = mtE/V$ [$\text{mtEU} \cdot \text{m}^{-3}$].

1242
 1243
 1244
 1245

1246 3.5. Evaluation of mitochondrial markers

1247

1248 Different methods are implicated in the quantification of mitochondrial markers and have
 1249 different strengths. Some problems are common for all mitochondrial markers, *mtE*: (1)
 1250 Accuracy of measurement is crucial, since even a highly accurate and reproducible
 1251 measurement of O₂ flux results in an inaccurate and noisy expression if normalized by a biased
 1252 and noisy measurement of a mitochondrial marker. This problem is acute in mitochondrial
 1253 respiration because the denominators used (the mitochondrial markers) are often small moieties
 1254 of which accurate and precise determination is difficult. This problem can be avoided when O₂
 1255 fluxes measured in substrate-uncoupler-inhibitor titration protocols are normalized for flux in
 1256 a defined respiratory reference state, which is used as an *internal* marker and yields flux control
 1257 ratios, *FCRs*. *FCRs* are independent of *externally* measured markers and, therefore, are
 1258 statistically robust, considering the limitations of ratios in general (Jasienski and Bazzaz 1999).
 1259 *FCRs* indicate qualitative changes of mitochondrial respiratory control, with highest
 1260 quantitative resolution, separating the effect of mitochondrial density or concentration on $J_{O_2/mX}$
 1261 and $I_{O_2/X}$ from that of function per elemental mitochondrial marker, $J_{O_2/mtE}$ (Pesta *et al.* 2011;
 1262 Gnaiger 2014). (2) If mitochondrial quality does not change and only the amount of
 1263 mitochondria varies as a determinant of mass-specific flux, any marker is equally qualified in
 1264 principle; then in practice selection of the optimum marker depends only on the accuracy and
 1265 precision of measurement of the mitochondrial marker. (3) If mitochondrial flux control ratios
 1266 change, then there may not be any best mitochondrial marker. In general, measurement of
 1267 multiple mitochondrial markers enables a comparison and evaluation of normalization for a
 1268 variety of mitochondrial markers. Particularly during postnatal development, the activity of
 1269 marker enzymes—such as cytochrome *c* oxidase and citrate synthase—follows different time
 1270 courses (Drahota *et al.* 2004). Evaluation of mitochondrial markers in healthy controls is
 1271 insufficient for providing guidelines for application in the diagnosis of pathological states and
 1272 specific treatments.

1273 In line with the concept of the respiratory control ratio (Chance and Williams 1955a), the
 1274 most readily used normalization is that of flux control ratios and flux control factors (Gnaiger
 1275 2014). Selection of the state of maximum flux in a protocol as the reference state has the
 1276 advantages of: (1) internal normalization; (2) statistically validated linearization of the response
 1277 in the range of 0 to 1; and (3) consideration of maximum flux for integrating a large number of
 1278 elemental steps in the OXPHOS- or ET-pathways. This reduces the risk of selecting a functional
 1279 marker that is specifically altered by the treatment or pathology, yet increases the chance that
 1280 the highly integrative pathway is disproportionately affected, *e.g.*, the OXPHOS- rather than
 1281 ET-pathway in case of an enzymatic defect in the phosphorylation-pathway. In this case,
 1282 additional information can be obtained by reporting flux control ratios based on a reference
 1283 state which indicates stable tissue-mass specific flux.

1284 Stereological determination of mitochondrial content via two-dimensional transmission
 1285 electron microscopy can have limitations due to the dynamics of mitochondrial size (Meinild
 1286 Lundby *et al.* 2017). Accurate determination of three-dimensional volume by two-dimensional
 1287 microscopy can be both time consuming and statistically challenging (Larsen *et al.* 2012).

1288 The validity of using mitochondrial marker enzymes (citrate synthase activity, Complex
 1289 I–IV amount or activity) for normalization of flux is limited in part by the same factors that
 1290 apply to flux control ratios. Strong correlations between various mitochondrial markers and
 1291 citrate synthase activity (Reichmann *et al.* 1985; Boushel *et al.* 2007; Mogensen *et al.* 2007)
 1292 are expected in a specific tissue of healthy persons and in disease states not specifically
 1293 targeting citrate synthase. Citrate synthase activity is acutely modifiable by exercise
 1294 (Tonkonogi *et al.* 1997; Leek *et al.* 2001). Evaluation of mitochondrial markers related to a
 1295 selected age and sex cohort cannot be extrapolated to provide recommendations for
 1296 normalization in respirometric diagnosis of disease, in different states of development and

1297 ageing, different cell types, tissues, and species. mtDNA normalized to nDNA via qPCR is
 1298 correlated to functional mitochondrial markers including OXPHOS- and ET-capacity in some
 1299 cases (Puntschart *et al.* 1995; Wang *et al.* 1999; Menshikova *et al.* 2006; Boushel *et al.* 2007),
 1300 but lack of such correlations have been reported (Menshikova *et al.* 2005; Schultz and Wiesner
 1301 2000; Pesta *et al.* 2011). Several studies indicate a strong correlation between cardiolipin
 1302 content and increase in mitochondrial function with exercise (Menshikova *et al.* 2005;
 1303 Menshikova *et al.* 2007; Larsen *et al.* 2012; Faber *et al.* 2014), but it has not been evaluated as
 1304 a general mitochondrial biomarker in disease. With no single best mitochondrial marker, a good
 1305 strategy is to quantify several different biomarkers to minimize the decorrelating effects caused
 1306 by diseases, treatments, or other factors. Determination of multiple markers, particularly a
 1307 matrix marker and a marker from the mtIM, allows tracking changes in mitochondrial quality
 1308 defined by their ratio.

1309

1310 3.6. Conversion: units

1311

1312 Many different units have been used to report the O₂ consumption rate, OCR (**Table 6**).
 1313 *SI* base units provide the common reference to introduce the theoretical principles (**Figure 7**),
 1314 and are used with appropriately chosen *SI* prefixes to express numerical data in the most
 1315 practical format, with an effort towards unification within specific areas of application (**Table**
 1316 **7**). Reporting data in *SI* units—including the mole [mol], coulomb [C], joule [J], and second
 1317 [s]—should be encouraged, particularly by journals which propose the use of *SI* units.

1318

1319

1320

1321

1322

1323

Table 6. Conversion of various units used in respirometry and ergometry. e^- is the number of electrons or reducing equivalents. z_B is the charge number of entity B.

1 Unit		Multiplication factor	<i>SI</i> -unit	Note
ng.atom O·s ⁻¹	(2 e ⁻)	0.5	nmol O ₂ ·s ⁻¹	
ng.atom O·min ⁻¹	(2 e ⁻)	8.33	pmol O ₂ ·s ⁻¹	
natom O·min ⁻¹	(2 e ⁻)	8.33	pmol O ₂ ·s ⁻¹	
nmol O ₂ ·min ⁻¹	(4 e ⁻)	16.67	pmol O ₂ ·s ⁻¹	
nmol O ₂ ·h ⁻¹	(4 e ⁻)	0.2778	pmol O ₂ ·s ⁻¹	
mL O ₂ ·min ⁻¹ at STPD ^a		0.744	μmol O ₂ ·s ⁻¹	1
W = J/s at -470 kJ/mol O ₂		-2.128	μmol O ₂ ·s ⁻¹	
mA = mC·s ⁻¹	($z_{H^+} = 1$)	10.36	nmol H ⁺ ·s ⁻¹	2
mA = mC·s ⁻¹	($z_{O_2} = 4$)	2.59	nmol O ₂ ·s ⁻¹	2
nmol H ⁺ ·s ⁻¹	($z_{H^+} = 1$)	0.09649	mA	3
nmol O ₂ ·s ⁻¹	($z_{O_2} = 4$)	0.38594	mA	3

1324

1325

1326

1327

1328

1329

1330

1331

1332

1 At standard temperature and pressure dry (STPD: 0 °C = 273.15 K and 1 atm = 101.325 kPa = 760 mmHg), the molar volume of an ideal gas, V_m , and V_{m,O_2} is 22.414 and 22.392 L·mol⁻¹, respectively. Rounded to three decimal places, both values yield the conversion factor of 0.744. For comparison at normal temperature and pressure dry (NTPD: 20 °C), V_{m,O_2} is 24.038 L·mol⁻¹. Note that the *SI* standard pressure is 100 kPa.

2 The multiplication factor is $10^6/(z_B \cdot F)$.

3 The multiplication factor is $z_B \cdot F/10^6$.

1333 Although volume is expressed as m^3 using the *SI* base unit, the litre [dm^3] is a
 1334 conventional unit of volume for concentration and is used for most solution chemical kinetics.
 1335 If one multiplies $I_{\text{O}_2/\text{cell}}$ by C_{Ncell} , then the result will not only be the amount of O_2 [mol]
 1336 consumed per time [s^{-1}] in one litre [L^{-1}], but also the change in O_2 concentration per second
 1337 (for any volume of an ideally closed system). This is ideal for kinetic modeling as it blends with
 1338 chemical rate equations where concentrations are typically expressed in $\text{mol}\cdot\text{L}^{-1}$ (Wagner *et al.*
 1339 2011). In studies of multinuclear cells—such as differentiated skeletal muscle cells—it is easy
 1340 to determine the number of nuclei but not the total number of cells. A generalized concept,
 1341 therefore, is obtained by substituting cells by nuclei as the sample entity. This does not hold,
 1342 however, for enucleated platelets.

1343 For studies of cells, we recommend that respiration be expressed, as far as possible, as:
 1344 (1) O_2 flux normalized for a mitochondrial marker, for separation of the effects of mitochondrial
 1345 quality and content on cell respiration (this includes *FCRs* as a normalization for a functional
 1346 mitochondrial marker); (2) O_2 flux in units of cell volume or mass, for comparison of respiration
 1347 of cells with different cell size (Renner *et al.* 2003) and with studies on tissue preparations, and
 1348 (3) O_2 flow in units of attomole (10^{-18} mol) of O_2 consumed in a second by each cell
 1349 [$\text{amol}\cdot\text{s}^{-1}\cdot\text{cell}^{-1}$], numerically equivalent to [$\text{pmol}\cdot\text{s}^{-1}\cdot 10^{-6}$ cells]. This convention allows
 1350 information to be easily used when designing experiments in which O_2 flow must be considered.
 1351 For example, to estimate the volume-specific O_2 flux in an instrument chamber that would be
 1352 expected at a particular cell number concentration, one simply needs to multiply the flow per
 1353 cell by the number of cells per volume of interest. This provides the amount of O_2 [mol]
 1354 consumed per time [s^{-1}] per unit volume [L^{-1}]. At an O_2 flow of $100 \text{ amol}\cdot\text{s}^{-1}\cdot\text{cell}^{-1}$ and a cell
 1355 density of $10^9 \text{ cells}\cdot\text{L}^{-1}$ ($10^6 \text{ cells}\cdot\text{mL}^{-1}$), the volume-specific O_2 flux is $100 \text{ nmol}\cdot\text{s}^{-1}\cdot\text{L}^{-1}$ (100
 1356 $\text{pmol}\cdot\text{s}^{-1}\cdot\text{mL}^{-1}$).

1357 **Table 7. Conversion of units with preservation of numerical values.**
 1358

Name	Frequently used unit	Equivalent unit	Note
volume-specific flux, J_{V,O_2}	$\text{pmol}\cdot\text{s}^{-1}\cdot\text{mL}^{-1}$	$\text{nmol}\cdot\text{s}^{-1}\cdot\text{L}^{-1}$	1
	$\text{mmol}\cdot\text{s}^{-1}\cdot\text{L}^{-1}$	$\text{mol}\cdot\text{s}^{-1}\cdot\text{m}^{-3}$	
cell-specific flow, $I_{\text{O}_2/\text{cell}}$	$\text{pmol}\cdot\text{s}^{-1}\cdot 10^{-6}$ cells	$\text{amol}\cdot\text{s}^{-1}\cdot\text{cell}^{-1}$	2
	$\text{pmol}\cdot\text{s}^{-1}\cdot 10^{-9}$ cells	$\text{zmol}\cdot\text{s}^{-1}\cdot\text{cell}^{-1}$	3
cell number concentration, C_{Nce}	$10^6 \text{ cells}\cdot\text{mL}^{-1}$	$10^9 \text{ cells}\cdot\text{L}^{-1}$	
mitochondrial protein concentration, C_{mtE}	$0.1 \text{ mg}\cdot\text{mL}^{-1}$	$0.1 \text{ g}\cdot\text{L}^{-1}$	
mass-specific flux, $J_{\text{O}_2/m}$	$\text{pmol}\cdot\text{s}^{-1}\cdot\text{mg}^{-1}$	$\text{nmol}\cdot\text{s}^{-1}\cdot\text{g}^{-1}$	4
catabolic power, P_k	$\mu\text{W}\cdot 10^{-6}$ cells	$\text{pW}\cdot\text{cell}^{-1}$	1
Volume	1,000 L	m^3 (1,000 kg)	
	L	dm^3 (kg)	
	mL	cm^3 (g)	
	μL	mm^3 (mg)	
	fL	μm^3 (pg)	5
amount of substance concentration	$\text{M} = \text{mol}\cdot\text{L}^{-1}$	$\text{mol}\cdot\text{dm}^{-3}$	

1359

1360 1 pmol: picomole = 10^{-12} mol 4 nmol: nanomole = 10^{-9} mol

1361 2 amol: attomole = 10^{-18} mol 5 fL: femtolitre = 10^{-15} L

1362 3 zmol: zeptomole = 10^{-21} mol

1363

1364 ET-capacity in human cell types including HEK 293, primary HUVEC and fibroblasts
 1365 ranges from 50 to $180 \text{ amol}\cdot\text{s}^{-1}\cdot\text{cell}^{-1}$, measured in intact cells in the noncoupled state (see
 1366 Gnaiger 2014). At $100 \text{ amol}\cdot\text{s}^{-1}\cdot\text{cell}^{-1}$ corrected for *Rox*, the current across the mt-membranes,

1367 I_{H^+e} , approximates 193 pA·cell⁻¹ or 0.2 nA per cell. See Rich (2003) for an extension of
1368 quantitative bioenergetics from the molecular to the human scale, with a transmembrane proton
1369 flux equivalent to 520 A in an adult at a catabolic power of -110 W. Modelling approaches
1370 illustrate the link between protonmotive force and currents (Willis *et al.* 2016).

1371 We consider isolated mitochondria as powerhouses and proton pumps as molecular
1372 machines to relate experimental results to energy metabolism of the intact cell. The cellular
1373 P_{\gg}/O_2 based on oxidation of glycogen is increased by the glycolytic (fermentative) substrate-
1374 level phosphorylation of 3 $P_{\gg}/Glyc$ or 0.5 mol P_{\gg} for each mol O_2 consumed in the complete
1375 oxidation of a mol glycosyl unit (Glyc). Adding 0.5 to the mitochondrial P_{\gg}/O_2 ratio of 5.4
1376 yields a bioenergetic cell physiological P_{\gg}/O_2 ratio close to 6. Two NADH equivalents are
1377 formed during glycolysis and transported from the cytosol into the mitochondrial matrix, either
1378 by the malate-aspartate shuttle or by the glycerophosphate shuttle (**Figure 2A**) resulting in
1379 different theoretical yields of ATP generated by mitochondria, the energetic cost of which
1380 potentially must be taken into account. Considering also substrate-level phosphorylation in the
1381 TCA cycle, this high P_{\gg}/O_2 ratio not only reflects proton translocation and OXPHOS studied
1382 in isolation, but integrates mitochondrial physiology with energy transformation in the living
1383 cell (Gnaiger 1993a).

1384
1385

1386 4. Conclusions

1387

1388 Catabolic cell respiration is the process of exergonic and exothermic energy
1389 transformation in which scalar redox reactions are coupled to vectorial ion translocation across
1390 a semipermeable membrane, which separates the small volume of a bacterial cell or
1391 mitochondrion from the larger volume of its surroundings. The electrochemical exergy can be
1392 partially conserved in the phosphorylation of ADP to ATP or in ion pumping, or dissipated in
1393 an electrochemical short-circuit. Respiration is thus clearly distinguished from fermentation as
1394 the counterpart of cellular core energy metabolism. An O_2 flux balance scheme illustrates the
1395 relationships and general definitions (**Figures 1 and 2**).

1396 Experimentally, respiration is separated in mitochondrial preparations from the
1397 interactions with the fermentative pathways of the intact cell. OXPHOS analysis (**Figure 3**) is
1398 based on the study of mitochondrial preparations complementary to bioenergetic investigations
1399 of intact cells and organisms—from model organisms to the human species including healthy
1400 and diseased persons (patients). Different mechanisms of respiratory uncoupling have to be
1401 distinguished (**Figure 4**). Metabolic fluxes measured in defined coupling and pathway control
1402 states (**Figures 5 and 6**) provide insights into the meaning of cellular and organismic
1403 respiration.

1404 The optimal choice for expressing mitochondrial and cell respiration as O_2 flow per
1405 biological sample, and normalization for specific tissue-markers (volume, mass, protein) and
1406 mitochondrial markers (volume, protein, content, mtDNA, activity of marker enzymes,
1407 respiratory reference state) is guided by the scientific question under study. Interpretation of
1408 the data depends critically on appropriate normalization (**Figure 7**).

1409 MitoEAGLE can serve as a gateway to better diagnose mitochondrial respiratory
1410 adaptations and defects linked to genetic variation, age-related health risks, sex-specific
1411 mitochondrial performance, lifestyle with its effects on degenerative diseases, and thermal and
1412 chemical environment. The present recommendations on coupling control states and rates,
1413 linked to the concept of the protonmotive force, are focused on studies with mitochondrial
1414 preparations (**Box 3**). These will be extended in a series of reports on pathway control of
1415 mitochondrial respiration, respiratory states in intact cells, and harmonization of experimental
1416 procedures.

1417

1418
1419
1420
1421
1422
1423
1424
1425
1426
1427
1428
1429
1430
1431
1432
1433
1434
1435
1436
1437
1438
1439
1440
1441
1442
1443
1444
1445
1446
1447
1448
1449
1450
1451
1452
1453
1454
1455
1456
1457
1458
1459
1460
1461
1462
1463
1464
1465
1466
1467
1468

Box 3: Recommendations for studies with mitochondrial preparations

- Normalization of respiratory rates should be provided as far as possible:
 1. *Biophysical normalization*: on a per cell basis as O₂ flow; this may not be possible when dealing with coenocytic organisms or tissues without cross-walls separating individual cells (*e.g.*, filamentous fungi, muscle fibers)
 2. *Cellular normalization*: per g protein; per cell- or tissue-mass as mass-specific O₂ flux; per cell volume as cell volume-specific flux
 3. *Mitochondrial normalization*: per mitochondrial marker as mt-specific flux.
 - With information on cell size and the use of multiple normalizations, maximum potential information is available (Renner *et al.* 2003; Wagner *et al.* 2011; Gnaiger 2014). Reporting flow in a respiratory chamber [nmol·s⁻¹] is discouraged, since it restricts the analysis to intra-experimental comparison of relative (qualitative) differences.
 - Catabolic mitochondrial respiration is distinguished from residual O₂ consumption. Fluxes in mitochondrial coupling states should be, as far as possible, corrected for residual O₂ consumption.
 - Different mechanisms of uncoupling should be distinguished by defined terms. The tightness of coupling relates to these uncoupling mechanisms, whereas the coupling stoichiometry varies as a function the substrate type involved in ET-pathways with either three or two redox proton pumps operating in series. Separation of tightness of coupling from the pathway-dependent coupling stoichiometry is possible only when the substrate type undergoing oxidation remains the same for respiration in LEAK-, OXPHOS-, and ET-states. In studies of the tightness of coupling, therefore, simple substrate-inhibitor combinations should be applied to exclude a shift in substrate competition which may occur when providing physiological substrate cocktails.
 - In studies of isolated mitochondria, the mitochondrial recovery and yield should be reported. Experimental criteria for evaluation of purity versus integrity should be considered. Mitochondrial markers—such as citrate synthase activity as an enzymatic matrix marker—provide a link to the tissue of origin on the basis of calculating the mitochondrial recovery, *i.e.*, the fraction of mitochondrial marker obtained from a unit mass of tissue. Total mitochondrial protein is frequently applied as a mitochondrial marker, which is restricted to isolated mitochondria.
 - In studies of permeabilized cells, the viability of the cell culture or cell suspension of origin should be reported. Normalization should be evaluated for total cell count or viable cell count.
 - Terms and symbols are summarized in **Table 8**. Their use will facilitate transdisciplinary communication and support further developments towards a consistent theory of bioenergetics and mitochondrial physiology. Technical terms related to and defined with normal words can be used as index terms in databases, support the creation of ontologies towards semantic information processing (MitoPedia), and help in communicating analytical findings as impactful data-driven stories. ‘*Making data available without making it understandable may be worse than not making it available at all*’ (National Academies of Sciences, Engineering, and Medicine 2018). Success will depend on taking next steps: (1) exhaustive text-mining considering Omics data and functional data; (2) network analysis of Omics data with bioinformatics tools; (3) cross-validation with distinct bioinformatics approaches; (4) correlation with functional data; (5) guidelines for biological validation of network data. This is a call to carefully contribute to FAIR principles (Findable, Accessible, Interoperable, Reusable) for the sharing of scientific data.
-

Table 8. Terms, symbols, and units.

Term	Symbol	Unit	Links and comments
alternative quinol oxidase	AOX		Figure 2B
amount of substance B	n_B	[mol]	
ATP yield per O ₂	$Y_{P\gg/O_2}$		P \gg /O ₂ ratio measured in any respiratory state
catabolic reaction	k		Figure 1 and 3
catabolic respiration	J_{kO_2}	<i>varies</i>	Figure 1 and 3
cell number	N_{cell}	[x]	Table 5; $N_{cell} = N_{vce} + N_{dce}$
cell respiration	J_{rO_2}	<i>varies</i>	Figure 1
cell viability index	CVI		$CVI = N_{vce}/N_{cell} = 1 - N_{dce}/N_{cell}$
Complexes I to IV	CI to CIV		respiratory ET Complexes; Figure 2B
concentration of substance B	$c_B = n_B \cdot V^{-1}$; [B]	[mol·m ⁻³]	Box 2
dead cell number	N_{dce}	[x]	Table 5; non-viable cells, loss of plasma membrane barrier function
electron transfer system	ETS		Figure 2B, Figure 5; state
flow, for substance B	I_B	[mol·s ⁻¹]	system-related extensive quantity; Figure 7
flux, for substance B	J_B	<i>varies</i>	size-specific quantity; Figure 7
inorganic phosphate	P _i		Figure 3
intact cell number, viable cell number	N_{vce}	[x]	Table 5; viable cells, intact of plasma membrane barrier function
LEAK	LEAK		Table 1, Figure 5; state
mass of sample X	m_X	[kg]	Table 4
mass of entity X	M_X	[kg]	mass of object X; Table 4
MITOCARTA			https://www.broadinstitute.org/scientific-community/science/programs/metabolic-disease-program/publications/mitocarta/mitocarta-in-0
MitoPedia			http://www.bioblast.at/index.php/MitoPedia
mitochondria or mitochondrial	mt		Box 1
mitochondrial DNA	mtDNA		Box 1
mitochondrial concentration	$C_{mtE} = mtE \cdot V^{-1}$	[mtEU·m ⁻³]	Table 4
mitochondrial content	$mtE_X = mtE \cdot N_X^{-1}$	[mtEU·x ⁻¹]	Table 4
mitochondrial elemental unit	mtEU	<i>varies</i>	Table 4, specific units for mt-marker
mitochondrial inner membrane	mtIM		Figure 2; MIM is widely used; the first M is replaced by mt; Box 1
mitochondrial outer membrane	mtOM		Figure 2; MOM is widely used; the first M is replaced by mt; Box 1
mitochondrial recovery	Y_{mtE}		fraction of <i>mtE</i> recovered in sample from the tissue of origin
mitochondrial yield	$Y_{mtE/m}$		$Y_{mtE/m} = Y_{mtE} \cdot D_{mtE}$
negative	neg		Figure 3
number concentration of X	C_{NX}	[x·m ⁻³]	Table 4
number of entities X	N_X	[x]	Table 4, Figure 7
number of entity B	N_B	[x]	Table 4
oxidative phosphorylation	OXPHOS		Table 1, Figure 5; state
oxygen concentration	$c_{O_2} = n_{O_2} \cdot V^{-1}$; [O ₂]	[mol·m ⁻³]	Section 3.2
oxygen flux, in reaction r	J_{rO_2}	<i>varies</i>	Figure 1
permeabilized cell number	N_{pce}	[x]	Table 5; experimental permeabilization of plasma membrane; $N_{pce} = N_{cell}$
phosphorylation of ADP to ATP	P \gg		Section 2.2
positive	pos		Figure 3
proton in the negative compartment	H ⁺ _{neg}		Figure 3
proton in the positive compartment	H ⁺ _{pos}		Figure 3
rate of electron transfer in ET state	E		ET-capacity; Table 1
rate of LEAK respiration	L		Table 1

1531	rate of oxidative phosphorylation	P		OXPPOS capacity; Table 1
1532	rate of residual oxygen consumption	R_{ox}		Table 1, Figure 1
1533	residual oxygen consumption	ROX		Table 1; state
1534	respiratory supercomplex	$SC I_n III_n IV_n$		Box 1; supramolecular assemblies composed of variable copy numbers (n) of CI, CIII and CIV
1535				
1536				
1537	specific mitochondrial density	$D_{mtE} = mtE \cdot m_X^{-1}$	[mtEU·kg ⁻¹]	Table 4
1538	volume	V	[m ³]	Table 7
1539	weight, dry weight	W_d	[kg]	used as mass of sample X; Figure 7
1540	weight, wet weight	W_w	[kg]	used as mass of sample X; Figure 7
1541				

1542

1543 Acknowledgements

1544 We thank M. Beno for management assistance. This publication is based upon work from COST
1545 Action CA15203 MitoEAGLE, supported by COST (European Cooperation in Science and
1546 Technology), and K-Regio project MitoFit (E.G.).

1547

1548 **Competing financial interests:** E.G. is founder and CEO of Oroboros Instruments, Innsbruck,
1549 Austria.

1550

1551 References

1552

- 1553 Altmann R (1894) Die Elementarorganismen und ihre Beziehungen zu den Zellen. Zweite vermehrte Auflage.
1554 Verlag Von Veit & Comp, Leipzig:160 pp.
- 1555 Beard DA (2005) A biophysical model of the mitochondrial respiratory system and oxidative phosphorylation.
1556 PLoS Comput Biol 1(4):e36.
- 1557 Benda C (1898) Weitere Mitteilungen über die Mitochondria. Verh Dtsch Physiol Ges:376-83.
- 1558 Birkedal R, Laasmaa M, Vendelin M (2014) The location of energetic compartments affects energetic
1559 communication in cardiomyocytes. Front Physiol 5:376.
- 1560 Blier PU, Dufresne F, Burton RS (2001) Natural selection and the evolution of mtDNA-encoded peptides:
1561 evidence for intergenomic co-adaptation. Trends Genet 17:400-6.
- 1562 Blier PU, Guderley HE (1993) Mitochondrial activity in rainbow trout red muscle: the effect of temperature on
1563 the ADP-dependence of ATP synthesis. J Exp Biol 176:145-58.
- 1564 Breton S, Beaupré HD, Stewart DT, Hoeh WR, Blier PU (2007) The unusual system of doubly uniparental
1565 inheritance of mtDNA: isn't one enough? Trends Genet 23:465-74.
- 1566 Brown GC (1992) Control of respiration and ATP synthesis in mammalian mitochondria and cells. Biochem J
1567 284:1-13.
- 1568 Calvo SE, Klauser CR, Mootha VK (2016) MitoCarta2.0: an updated inventory of mammalian mitochondrial
1569 proteins. Nucleic Acids Research 44:D1251-7.
- 1570 Calvo SE, Julien O, Clauser KR, Shen H, Kamer KJ, Wells JA, Mootha VK (2017) Comparative analysis of
1571 mitochondrial N-termini from mouse, human, and yeast. Mol Cell Proteomics 16:512-23.
- 1572 Campos JC, Queliconi BB, Bozi LHM, Bechara LRG, Dourado PMM, Andres AM, Jannig PR, Gomes KMS,
1573 Zambelli VO, Rocha-Resende C, Guatimosim S, Brum PC, Mochly-Rosen D, Gottlieb RA, Kowaltowski AJ,
1574 Ferreira JCB (2017) Exercise reestablishes autophagic flux and mitochondrial quality control in heart failure.
1575 Autophagy 13:1304-317.
- 1576 Canton M, Luvisetto S, Schmehl I, Azzone GF (1995) The nature of mitochondrial respiration and
1577 discrimination between membrane and pump properties. Biochem J 310:477-81.
- 1578 Carrico C, Meyer JG, He W, Gibson BW, Verdin E (2018) The mitochondrial acylome emerges: proteomics,
1579 regulation by Sirtuins, and metabolic and disease implications. Cell Metab 27:497-512.
- 1580 Chan DC (2006) Mitochondria: dynamic organelles in disease, aging, and development. Cell 125:1241-52.
- 1581 Chance B, Williams GR (1955a) Respiratory enzymes in oxidative phosphorylation. I. Kinetics of oxygen
1582 utilization. J Biol Chem 217:383-93.
- 1583 Chance B, Williams GR (1955b) Respiratory enzymes in oxidative phosphorylation: III. The steady state. J Biol
1584 Chem 217:409-27.
- 1585 Chance B, Williams GR (1955c) Respiratory enzymes in oxidative phosphorylation. IV. The respiratory chain. J
1586 Biol Chem 217:429-38.
- 1587 Chance B, Williams GR (1956) The respiratory chain and oxidative phosphorylation. Adv Enzymol Relat Subj
1588 Biochem 17:65-134.

- 1589 Chowdhury SK, Djordjevic J, Albensi B, Fernyhough P (2015) Simultaneous evaluation of substrate-dependent
1590 oxygen consumption rates and mitochondrial membrane potential by TMRM and safranin in cortical
1591 mitochondria. *Biosci Rep* 36:e00286.
- 1592 Cobb LJ, Lee C, Xiao J, Yen K, Wong RG, Nakamura HK, Mehta HH, Gao Q, Ashur C, Huffman DM, Wan J,
1593 Muzumdar R, Barzilai N, Cohen P (2016) Naturally occurring mitochondrial-derived peptides are age-
1594 dependent regulators of apoptosis, insulin sensitivity, and inflammatory markers. *Aging (Albany NY)* 8:796-
1595 809.
- 1596 Cohen ER, Cvitas T, Frey JG, Holmström B, Kuchitsu K, Marquardt R, Mills I, Pavese F, Quack M, Stohner J,
1597 Strauss HL, Takami M, Thor HL (2008) Quantities, units and symbols in physical chemistry, IUPAC Green
1598 Book, 3rd Edition, 2nd Printing, IUPAC & RSC Publishing, Cambridge.
- 1599 Cooper H, Hedges LV, Valentine JC, eds (2009) *The handbook of research synthesis and meta-analysis*. Russell
1600 Sage Foundation.
- 1601 Coopersmith J (2010) *Energy, the subtle concept. The discovery of Feynman's blocks from Leibnitz to Einstein*.
1602 Oxford University Press:400 pp.
- 1603 Cummins J (1998) Mitochondrial DNA in mammalian reproduction. *Rev Reprod* 3:172-82.
- 1604 Dai Q, Shah AA, Garde RV, Yonish BA, Zhang L, Medvitz NA, Miller SE, Hansen EL, Dunn CN, Price TM
1605 (2013) A truncated progesterone receptor (PR-M) localizes to the mitochondrion and controls cellular
1606 respiration. *Mol Endocrinol* 27:741-53.
- 1607 Daum B, Walter A, Horst A, Osiewacz HD, Kühlbrandt W (2013) Age-dependent dissociation of ATP synthase
1608 dimers and loss of inner-membrane cristae in mitochondria. *Proc Natl Acad Sci U S A* 110:15301-6.
- 1609 Divakaruni AS, Brand MD (2011) The regulation and physiology of mitochondrial proton leak. *Physiology*
1610 (Bethesda) 26:192-205.
- 1611 Doerrier C, Garcia-Souza LF, Krumschnabel G, Wohlfarter Y, Mészáros AT, Gnaiger E (2018) High-Resolution
1612 Fluorescence Respirometry and OXPHOS protocols for human cells, permeabilized fibres from small biopsies of
1613 muscle, and isolated mitochondria. *Methods Mol Biol* 1782 (Palmeira CM, Moreno AJ, eds): Mitochondrial
1614 Bioenergetics, 978-1-4939-7830-4.
- 1615 Doskey CM, van 't Erve TJ, Wagner BA, Buettner GR (2015) Moles of a substance per cell is a highly
1616 informative dosing metric in cell culture. *PLOS ONE* 10:e0132572.
- 1617 Drahotová Z, Milerová M, Stieglerová A, Houstek J, Ostádal B (2004) Developmental changes of cytochrome *c*
1618 oxidase and citrate synthase in rat heart homogenate. *Physiol Res* 53:119-22.
- 1619 Duarte FV, Palmeira CM, Rolo AP (2014) The role of microRNAs in mitochondria: small players acting wide.
1620 *Genes (Basel)* 5:865-86.
- 1621 Ernster L, Schatz G (1981) Mitochondria: a historical review. *J Cell Biol* 91:227s-55s.
- 1622 Estabrook RW (1967) Mitochondrial respiratory control and the polarographic measurement of ADP:O ratios.
1623 *Methods Enzymol* 10:41-7.
- 1624 Faber C, Zhu ZJ, Castellino S, Wagner DS, Brown RH, Peterson RA, Gates L, Barton J, Bickett M, Hagerty L,
1625 Kimbrough C, Sola M, Bailey D, Jordan H, Elangbam CS (2014) Cardiolipin profiles as a potential
1626 biomarker of mitochondrial health in diet-induced obese mice subjected to exercise, diet-restriction and
1627 ephedrine treatment. *J Appl Toxicol* 34:1122-9.
- 1628 Fell D (1997) *Understanding the control of metabolism*. Portland Press.
- 1629 Garlid KD, Beavis AD, Ratkje SK (1989) On the nature of ion leaks in energy-transducing membranes. *Biochim*
1630 *Biophys Acta* 976:109-20.
- 1631 Garlid KD, Semrad C, Zinchenko V. Does redox slip contribute significantly to mitochondrial respiration? In:
1632 Schuster S, Rigoulet M, Ouhabi R, Mazat J-P, eds (1993) *Modern trends in biothermokinetics*. Plenum Press,
1633 New York, London:287-93.
- 1634 Gerö D, Szabo C (2016) Glucocorticoids suppress mitochondrial oxidant production via upregulation of
1635 uncoupling protein 2 in hyperglycemic endothelial cells. *PLoS One* 11:e0154813.
- 1636 Gnaiger E. Efficiency and power strategies under hypoxia. Is low efficiency at high glycolytic ATP production a
1637 paradox? In: *Surviving Hypoxia: Mechanisms of Control and Adaptation*. Hochachka PW, Lutz PL, Sick T,
1638 Rosenthal M, Van den Thillart G, eds (1993a) CRC Press, Boca Raton, Ann Arbor, London, Tokyo:77-109.
- 1639 Gnaiger E (1993b) Nonequilibrium thermodynamics of energy transformations. *Pure Appl Chem* 65:1983-2002.
- 1640 Gnaiger E (2001) Bioenergetics at low oxygen: dependence of respiration and phosphorylation on oxygen and
1641 adenosine diphosphate supply. *Respir Physiol* 128:277-97.
- 1642 Gnaiger E (2009) Capacity of oxidative phosphorylation in human skeletal muscle. *New perspectives of*
1643 *mitochondrial physiology*. *Int J Biochem Cell Biol* 41:1837-45.
- 1644 Gnaiger E (2014) *Mitochondrial pathways and respiratory control. An introduction to OXPHOS analysis*. 4th ed.
1645 *Mitochondr Physiol Network* 19.12. Oroboros MiPNet Publications, Innsbruck:80 pp.
- 1646 Gnaiger E, Méndez G, Hand SC (2000) High phosphorylation efficiency and depression of uncoupled respiration
1647 in mitochondria under hypoxia. *Proc Natl Acad Sci USA* 97:11080-5.
- 1648 Greggio C, Jha P, Kulkarni SS, Lagarrigue S, Broskey NT, Boutant M, Wang X, Conde Alonso S, Ofori E,
1649 Auwerx J, Cantó C, Amati F (2017) Enhanced respiratory chain supercomplex formation in response to
1650 exercise in human skeletal muscle. *Cell Metab* 25:301-11.

- 1651 Hinkle PC (2005) P/O ratios of mitochondrial oxidative phosphorylation. *Biochim Biophys Acta* 1706:1-11.
- 1652 Hofstadter DR (1979) Gödel, Escher, Bach: An eternal golden braid. A metaphorical fugue on minds and
1653 machines in the spirit of Lewis Carroll. Harvester Press:499 pp.
- 1654 Illaste A, Laasmaa M, Peterson P, Vendelin M (2012) Analysis of molecular movement reveals latticelike
1655 obstructions to diffusion in heart muscle cells. *Biophys J* 102:739-48.
- 1656 Jasienski M, Bazzaz FA (1999) The fallacy of ratios and the testability of models in biology. *Oikos* 84:321-26.
- 1657 Jepihhina N, Beraud N, Sepp M, Birkedal R, Vendelin M (2011) Permeabilized rat cardiomyocyte response
1658 demonstrates intracellular origin of diffusion obstacles. *Biophys J* 101:2112-21.
- 1659 Klepinin A, Ounpuu L, Guzun R, Chekulayev V, Timohhina N, Tepp K, Shevchuk I, Schlattner U, Kaambre T
1660 (2016) Simple oxygraphic analysis for the presence of adenylate kinase 1 and 2 in normal and tumor cells. *J*
1661 *Bioenerg Biomembr* 48:531-48.
- 1662 Klingenberg M (2017) UCP1 - A sophisticated energy valve. *Biochimie* 134:19-27.
- 1663 Koit A, Shevchuk I, Ounpuu L, Klepinin A, Chekulayev V, Timohhina N, Tepp K, Puurand M, Truu L, Heck K,
1664 Valvere V, Guzun R, Kaambre T (2017) Mitochondrial respiration in human colorectal and breast cancer
1665 clinical material is regulated differently. *Oxid Med Cell Longev* 1372640.
- 1666 Komlódi T, Tretter L (2017) Methylene blue stimulates substrate-level phosphorylation catalysed by succinyl-
1667 CoA ligase in the citric acid cycle. *Neuropharmacology* 123:287-98.
- 1668 Lane N (2005) Power, sex, suicide: mitochondria and the meaning of life. Oxford University Press:354 pp.
- 1669 Larsen S, Nielsen J, Neigaard Nielsen C, Nielsen LB, Wibrand F, Stride N, Schroder HD, Boushel RC, Helge
1670 JW, Dela F, Hey-Mogensen M (2012) Biomarkers of mitochondrial content in skeletal muscle of healthy
1671 young human subjects. *J Physiol* 590:3349-60.
- 1672 Lee C, Zeng J, Drew BG, Sallam T, Martin-Montalvo A, Wan J, Kim SJ, Mehta H, Hevener AL, de Cabo R,
1673 Cohen P (2015) The mitochondrial-derived peptide MOTS-c promotes metabolic homeostasis and reduces
1674 obesity and insulin resistance. *Cell Metab* 21:443-54.
- 1675 Lee SR, Kim HK, Song IS, Youm J, Dizon LA, Jeong SH, Ko TH, Heo HJ, Ko KS, Rhee BD, Kim N, Han J
1676 (2013) Glucocorticoids and their receptors: insights into specific roles in mitochondria. *Prog Biophys Mol*
1677 *Biol* 112:44-54.
- 1678 Leek BT, Mudaliar SR, Henry R, Mathieu-Costello O, Richardson RS (2001) Effect of acute exercise on citrate
1679 synthase activity in untrained and trained human skeletal muscle. *Am J Physiol Regul Integr Comp Physiol*
1680 280:R441-7.
- 1681 Lemieux H, Blier PU, Gnaiger E (2017) Remodeling pathway control of mitochondrial respiratory capacity by
1682 temperature in mouse heart: electron flow through the Q-junction in permeabilized fibers. *Sci Rep* 7:2840.
- 1683 Lenaz G, Tioli G, Falasca AI, Genova ML (2017) Respiratory supercomplexes in mitochondria. In: Mechanisms
1684 of primary energy trasduction in biology. M Wikstrom (ed) Royal Society of Chemistry Publishing, London,
1685 UK:296-337.
- 1686 Liu S, Roellig DM, Guo Y, Li N, Frace MA, Tang K, Zhang L, Feng Y, Xiao L (2016) Evolution of mitosome
1687 metabolism and invasion-related proteins in *Cryptosporidium*. *BMC Genomics* 17:1006.
- 1688 Margulis L (1970) Origin of eukaryotic cells. New Haven: Yale University Press.
- 1689 Meinild Lundby AK, Jacobs RA, Gehrig S, de Leur J, Hauser M, Bonne TC, Flück D, Dandanell S, Kirk N,
1690 Kaech A, Ziegler U, Larsen S, Lundby C (2018) Exercise training increases skeletal muscle mitochondrial
1691 volume density by enlargement of existing mitochondria and not de novo biogenesis. *Acta Physiol* 222,
1692 e12905.
- 1693 Menshikova EV, Ritov VB, Fairfull L, Ferrell RE, Kelley DE, Goodpaster BH (2006) Effects of exercise on
1694 mitochondrial content and function in aging human skeletal muscle. *J Gerontol A Biol Sci Med Sci* 61:534-
1695 40.
- 1696 Menshikova EV, Ritov VB, Ferrell RE, Azuma K, Goodpaster BH, Kelley DE (2007) Characteristics of skeletal
1697 muscle mitochondrial biogenesis induced by moderate-intensity exercise and weight loss in obesity. *J Appl*
1698 *Physiol* (1985) 103:21-7.
- 1699 Menshikova EV, Ritov VB, Toledo FG, Ferrell RE, Goodpaster BH, Kelley DE (2005) Effects of weight loss
1700 and physical activity on skeletal muscle mitochondrial function in obesity. *Am J Physiol Endocrinol Metab*
1701 288:E818-25.
- 1702 Miller GA (1991) The science of words. Scientific American Library New York:276 pp.
- 1703 Mitchell P (1961) Coupling of phosphorylation to electron and hydrogen transfer by a chemi-osmotic type of
1704 mechanism. *Nature* 191:144-8.
- 1705 Mitchell P (2011) Chemiosmotic coupling in oxidative and photosynthetic phosphorylation. *Biochim Biophys*
1706 *Acta Bioenergetics* 1807:1507-38.
- 1707 Mogensen M, Sahlin K, Fernström M, Glintborg D, Vind BF, Beck-Nielsen H, Højlund K (2007) Mitochondrial
1708 respiration is decreased in skeletal muscle of patients with type 2 diabetes. *Diabetes* 56:1592-9.
- 1709 Mohr PJ, Phillips WD (2015) Dimensionless units in the SI. *Metrologia* 52:40-7.
- 1710 Moreno M, Giacco A, Di Munno C, Goglia F (2017) Direct and rapid effects of 3,5-diiodo-L-thyronine (T2).
1711 *Mol Cell Endocrinol* 7207:30092-8.

- 1712 Morrow RM, Picard M, Derbeneva O, Leipzig J, McManus MJ, Gousspillou G, Barbat-Artigas S, Dos Santos C,
 1713 Hepple RT, Murdock DG, Wallace DC (2017) Mitochondrial energy deficiency leads to hyperproliferation of
 1714 skeletal muscle mitochondria and enhanced insulin sensitivity. *Proc Natl Acad Sci U S A* 114:2705-10.
- 1715 Murley A, Nunnari J (2016) The emerging network of mitochondria-organelle contacts. *Mol Cell* 61:648-53.
- 1716 National Academies of Sciences, Engineering, and Medicine (2018) International coordination for science data
 1717 infrastructure: Proceedings of a workshop—in brief. Washington, DC: The National Academies Press. doi:
 1718 <https://doi.org/10.17226/25015>.
- 1719 Palmfeldt J, Bross P (2017) Proteomics of human mitochondria. *Mitochondrion* 33:2-14.
- 1720 Paradies G, Paradies V, De Benedictis V, Ruggiero FM, Petrosillo G (2014) Functional role of cardiolipin in
 1721 mitochondrial bioenergetics. *Biochim Biophys Acta* 1837:408-17.
- 1722 Pesta D, Gnaiger E (2012) High-Resolution Respirometry. OXPHOS protocols for human cells and
 1723 permeabilized fibres from small biopsies of human muscle. *Methods Mol Biol* 810:25-58.
- 1724 Pesta D, Hoppel F, Macek C, Messner H, Faulhaber M, Kobel C, Parson W, Burtscher M, Schocke M, Gnaiger
 1725 E (2011) Similar qualitative and quantitative changes of mitochondrial respiration following strength and
 1726 endurance training in normoxia and hypoxia in sedentary humans. *Am J Physiol Regul Integr Comp Physiol*
 1727 301:R1078–87.
- 1728 Price TM, Dai Q (2015) The role of a mitochondrial progesterone receptor (PR-M) in progesterone action.
 1729 *Semin Reprod Med* 33:185-94.
- 1730 Puchowicz MA, Varnes ME, Cohen BH, Friedman NR, Kerr DS, Hoppel CL (2004) Oxidative phosphorylation
 1731 analysis: assessing the integrated functional activity of human skeletal muscle mitochondria – case studies.
 1732 *Mitochondrion* 4:377-85. Puntschart A, Claassen H, Jostarndt K, Hoppeler H, Billeter R (1995) mRNAs of
 1733 enzymes involved in energy metabolism and mtDNA are increased in endurance-trained athletes. *Am J*
 1734 *Physiol* 269:C619-25.
- 1735 Quiros PM, Mottis A, Auwerx J (2016) Mitonuclear communication in homeostasis and stress. *Nat Rev Mol*
 1736 *Cell Biol* 17:213-26.
- 1737 Rackham O, Mercer TR, Filipovska A (2012) The human mitochondrial transcriptome and the RNA-binding
 1738 proteins that regulate its expression. *WIREs RNA* 3:675–95.
- 1739 Reichmann H, Hoppeler H, Mathieu-Costello O, von Bergen F, Pette D (1985) Biochemical and ultrastructural
 1740 changes of skeletal muscle mitochondria after chronic electrical stimulation in rabbits. *Pflugers Arch* 404:1-
 1741 9.
- 1742 Renner K, Amberger A, Konwalinka G, Gnaiger E (2003) Changes of mitochondrial respiration, mitochondrial
 1743 content and cell size after induction of apoptosis in leukemia cells. *Biochim Biophys Acta* 1642:115-23.
- 1744 Rice DW, Alverson AJ, Richardson AO, Young GJ, Sanchez-Puerta MV, Munzinger J, Barry K, Boore JL,
 1745 Zhang Y, dePamphilis CW, Knox EB, Palmer JD (2016) Horizontal transfer of entire genomes via
 1746 mitochondrial fusion in the angiosperm *Amborella*. *Science* 342:1468-73.
- 1747 Rich P (2003) Chemiosmotic coupling: The cost of living. *Nature* 421:583.
- 1748 Rostovtseva TK, Sheldon KL, Hassanzadeh E, Monge C, Saks V, Bezrukov SM, Sackett DL (2008) Tubulin
 1749 binding blocks mitochondrial voltage-dependent anion channel and regulates respiration. *Proc Natl Acad Sci*
 1750 *USA* 105:18746-51.
- 1751 Rustin P, Parfait B, Chretien D, Bourgeron T, Djouadi F, Bastin J, Rötig A, Munnich A (1996) Fluxes of
 1752 nicotinamide adenine dinucleotides through mitochondrial membranes in human cultured cells. *J Biol Chem*
 1753 271:14785-90.
- 1754 Saks VA, Veksler VI, Kuznetsov AV, Kay L, Sikk P, Tiivel T, Tranqui L, Olivares J, Winkler K, Wiedemann F,
 1755 Kunz WS (1998) Permeabilised cell and skinned fiber techniques in studies of mitochondrial function in
 1756 vivo. *Mol Cell Biochem* 184:81-100.
- 1757 Salabei JK, Gibb AA, Hill BG (2014) Comprehensive measurement of respiratory activity in permeabilized cells
 1758 using extracellular flux analysis. *Nat Protoc* 9:421-38.
- 1759 Sazanov LA (2015) A giant molecular proton pump: structure and mechanism of respiratory complex I. *Nat Rev*
 1760 *Mol Cell Biol* 16:375-88.
- 1761 Schneider TD (2006) Claude Shannon: biologist. The founder of information theory used biology to formulate
 1762 the channel capacity. *IEEE Eng Med Biol Mag* 25:30-3.
- 1763 Schönfeld P, Dymkowska D, Wojtczak L (2009) Acyl-CoA-induced generation of reactive oxygen species in
 1764 mitochondrial preparations is due to the presence of peroxisomes. *Free Radic Biol Med* 47:503-9.
- 1765 Schultz J, Wiesner RJ (2000) Proliferation of mitochondria in chronically stimulated rabbit skeletal muscle--
 1766 transcription of mitochondrial genes and copy number of mitochondrial DNA. *J Bioenerg Biomembr* 32:627-
 1767 34.
- 1768 Speijer D (2016) Being right on Q: shaping eukaryotic evolution. *Biochem J* 473:4103-27.
- 1769 Sugiura A, Mattie S, Prudent J, McBride HM (2017) Newly born peroxisomes are a hybrid of mitochondrial and
 1770 ER-derived pre-peroxisomes. *Nature* 542:251-4.
- 1771 Simson P, Jephthina N, Laasmaa M, Peterson P, Birkedal R, Vendelin M (2016) Restricted ADP movement in
 1772 cardiomyocytes: Cytosolic diffusion obstacles are complemented with a small number of open mitochondrial
 1773 voltage-dependent anion channels. *J Mol Cell Cardiol* 97:197-203.

- 1774 Stucki JW, Ineichen EA (1974) Energy dissipation by calcium recycling and the efficiency of calcium transport
1775 in rat-liver mitochondria. *Eur J Biochem* 48:365-75.
- 1776 Tonkonogi M, Harris B, Sahlin K (1997) Increased activity of citrate synthase in human skeletal muscle after a
1777 single bout of prolonged exercise. *Acta Physiol Scand* 161:435-6.
- 1778 Torralba D, Baixauli F, Sánchez-Madrid F (2016) Mitochondria know no boundaries: mechanisms and functions
1779 of intercellular mitochondrial transfer. *Front Cell Dev Biol* 4:107. eCollection 2016.
- 1780 Vamecq J, Schepers L, Parmentier G, Mannaerts GP (1987) Inhibition of peroxisomal fatty acyl-CoA oxidase by
1781 antimycin A. *Biochem J* 248:603-7.
- 1782 Waczulikova I, Habodaszova D, Cagalinec M, Ferko M, Ulicna O, Mateasik A, Sikurova L, Ziegelhöffer A
1783 (2007) Mitochondrial membrane fluidity, potential, and calcium transients in the myocardium from acute
1784 diabetic rats. *Can J Physiol Pharmacol* 85:372-81.
- 1785 Wagner BA, Venkataraman S, Buettner GR (2011) The rate of oxygen utilization by cells. *Free Radic Biol Med*
1786 51:700-712.
- 1787 Wang H, Hiatt WR, Barstow TJ, Brass EP (1999) Relationships between muscle mitochondrial DNA content,
1788 mitochondrial enzyme activity and oxidative capacity in man: alterations with disease. *Eur J Appl Physiol*
1789 *Occup Physiol* 80:22-7.
- 1790 Watt IN, Montgomery MG, Runswick MJ, Leslie AG, Walker JE (2010) Bioenergetic cost of making an
1791 adenosine triphosphate molecule in animal mitochondria. *Proc Natl Acad Sci U S A* 107:16823-7.
- 1792 Weibel ER, Hoppeler H (2005) Exercise-induced maximal metabolic rate scales with muscle aerobic capacity. *J*
1793 *Exp Biol* 208:1635-44.
- 1794 White DJ, Wolff JN, Pierson M, Gemmell NJ (2008) Revealing the hidden complexities of mtDNA inheritance.
1795 *Mol Ecol* 17:4925-42.
- 1796 Wikström M, Hummer G (2012) Stoichiometry of proton translocation by respiratory complex I and its
1797 mechanistic implications. *Proc Natl Acad Sci U S A* 109:4431-6.
- 1798 Williams EG, Wu Y, Jha P, Dubuis S, Blattmann P, Argmann CA, Houten SM, Amariuta T, Wolski W,
1799 Zamboni N, Aebersold R, Auwerx J (2016) Systems proteomics of liver mitochondria function. *Science* 352
1800 (6291):aad0189
- 1801 Willis WT, Jackman MR, Messer JI, Kuzmiak-Glancy S, Glancy B (2016) A simple hydraulic analog model of
1802 oxidative phosphorylation. *Med Sci Sports Exerc* 48:990-1000.
- 1803